

AD-A149 786 AN INVESTIGATION OF TURBULENCE MECHANISMS IN V/STOL 1/1

AD-A149 786 AN INVESTIGATION OF TURBULENCE MECHANISMS IN V/STOL 1/1

AD-A149 786 AN INVESTIGATION OF TURBULENCE MECHANISMS IN V/STOL 1/1

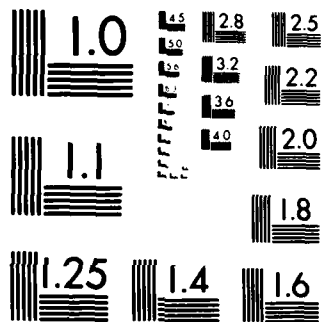
UNCLASSIFIED RE-688 AFOSR-TR-84-1197 F49620-82-C-0025 F/G 20/4 NL

UNCLASSIFIED RE-688 AFOSR-TR-84-1197 F49620-82-C-0025 F/G 20/4 NL

UNCLASSIFIED RE-688 AFOSR-TR-84-1197 F49620-82-C-0025 F/G 20/4 NL

UNCLASSIFIED RE-688 AFOSR-TR-84-1197 F49620-82-C-0025 F/G 20/4 NL

4. 10. 1974



MICROCOPY RESOLUTION TEST CHART
NATIONAL BUREAU OF STANDARDS-1963-A



AFOSR-TR- 84-1197

REPORT RE-688

AN INVESTIGATION OF TURBULENCE MECHANISMS
IN V/STOL UPWASH FLOW FIELDS

August 1984

prepared by

Barry L. Gilbert
Aerosciences Directorate

Research and Development Center
Grumman Aerospace Corporation
Bethpage, New York 11714

Second Annual Report on
Contract F49620-82-C-0025
For the period March 15, 1983 through June 15, 1984

prepared for

Dr. James D. Wilson
External Aerodynamics and Fluid Mechanics
Air Force Office of Scientific Research
Bolling AFB, Washington D.C. 20332

AFOSR-TR-84-1197
RE-688
DISTRIBUTION STATEMENT A
Approved for public release
Distribution Unlimited
Chief, Technical Division

Approved by:

Richard A. Scheuing
Richard A. Scheuing, V.P.
Director, R&D Center

DISTRIBUTION STATEMENT A

Approved for public release
Distribution Unlimited

CONTENTS

<u>Section</u>	<u>Page</u>
ABSTRACT.....	1
RESEARCH OBJECTIVES.....	3
SIGNIFICANT ACCOMPLISHMENTS.....	5
Summary.....	5
Wall Jet.....	6
Equal Jet Upwash.....	14
Unequal Wall Jets.....	27
Unequal Jet Analysis.....	35
Centerline Obstacles.....	41
Radial Wall Jets.....	42
Conclusion.....	48
REFERENCES.....	49
PUBLICATION FROM THIS CONTRACT.....	51
PERSONNEL.....	51

Accession For	
NTIS GPO	<input checked="" type="checkbox"/>
DTIC TAB	<input type="checkbox"/>
Unannounced	<input type="checkbox"/>
Justification	
By	
Distribution/	
Availability Codes	
Dist	Qual and/or
A-1	Special



LIST OF ILLUSTRATIONS

<u>Figure</u>		<u>Page</u>
1	Diagram of Two-dimensional Jet Upwash Facility.....	7
2	Photograph of Two-dimensional Jet Upwash Facility.....	8
3	Coordinate System Nomenclature Conversion.....	10
4	Typical Jet Exit Velocity Profiles.....	11
5	Two-dimensional Wall Jet Characteristics.....	12
6	Wall Jet Mean Velocity Profiles in Similarity Form.....	13
7	Wall Jet Turbulence Intensity Profiles in Similar Form.....	13
8	Upwash Flow Field Vectors for Equal Wall Jets at Seven Heights.....	16
9	Spread Rate and Mean Velocity Decay in a Two-dimensional Upwash.....	18
10	Mean Velocity Profiles for Equal Wall Jet Upwash at Six Heights in Similarity Form.....	20
11	Component Turbulent Energy in the Mean Flow Direction at Six Heights.....	20
12	Component Turbulence Energy in the Cross Flow Direction at Six Heights.....	21
13	Component Turbulence Energy in the Third Orthogonal Direction at Six Heights.....	21
14	Total Turbulence Kinetic Energy in an Equal Wall Jet Upwash at Six Heights.....	22
15	Ratio of the Cross Component Turbulence Energy.....	22
16	Shear Stress Component in an Upwash at Six Heights.....	24
17	Intermittency Profiles in an Equal Jet Upwash.....	24
18	Comparison of Mean and Turbulence Profiles for a Free 2-D Jet with a 2-D Upwash.....	25
19	Integral Scale Lengths Across 2-D Upwash.....	26
20	Taylor Micro-scale Lengths Across 2-D Upwash.....	26

LIST OF ILLUSTRATIONS (continued)

<u>Figure</u>		<u>Page</u>
21	Upwash Flow Field Vectors for Pressure Ratio = 1.0.....	28
22	Upwash Flow Field Vectors for Pressure Ratio = 1.2.....	29
23	Upwash Flow Field Vectors for Pressure Ratio = 1.4.....	30
24	Upwash Flow Field Vectors for Pressure Ratio = 1.6.....	31
25	Upwash Flow Field Vectors for Pressure Ratio = 1.8.....	32
26	Half Velocity Width Growth Rate in the Upwash of Unequal Wall Jets.....	33
27	Mean Velocity Decay in the Upwash of Unequal Wall Jets.....	33
28	Position of the Maximum Velocity Peak in the Upwash of Unequal Wall Jets.....	34
29	Turbulence Kinetic Energy in the Upwash of Unequal Wall Jets.....	36
30	Unequal Wall Jet Diagram.....	38
31	Diagram of New Radial Wall Jet Design.....	44
32	Radial Wall Jet Exit Profiles.....	45
33	Radial Wall Jet Mean Velocity Decay Profile.....	46
34	Radial Wall Jet Momentum for Different Gap Heights.....	46
35	Increased Mass Flow Rate for Radial Wall Jets.....	47
36	Radial Wall Jets Mean Velocity Profiles.....	47

ABSTRACT

Presented are the results of the first two years of an experimental investigation of the abnormally high turbulent mixing layer growth rate characteristics found in the upwash regions of V/STOL flows in ground effect. The overall objectives of this program are to examine the origin of the increased fluctuations, to characterize systematically the development and structure of the upwash, and to determine the parameters that influence these characteristics. The approach adopted is to investigate the fundamental turbulent V/STOL upwash mechanisms in increasingly more complex flow configurations.

Most of this study utilizes the two-dimensional upwash formed by the collision of opposed two-dimensional wall jets. Extensive measurements have been made in the two-dimensional wall jet to establish the starting conditions of the upwash. Evaluation of these measurements has shown classical wall jet behavior, and fully developed mean and turbulence profiles at the collision zone.

A unique set of velocity profiles was obtained at seven locations in the upwash. Two components of the velocity were found simultaneously using an X-probe anemometer. By rotating the probe and repeating the profiles, all three velocity components were measured. This baseline set of component velocity profiles has never been reported before. While mixing layer growth rates were larger than those found in a free two-dimensional jet, these values were less than those reported by previous investigators. The abnormally high turbulence levels reported by other investigators were not found. These data are presented in similarity form. Higher moments and some of the terms in the turbulence kinetic energy equation were also measured.

As part of the study of the effect of various initial conditions, a series of measurements was taken in the upwash region formed by the collision of unequal wall jets. These are compared to a very simple theory. By choosing a coordinate system aligned with the upwash, these data can be characterized in a pattern similar to the equal wall jet case. Obstacles of various heights were placed at the collision point of equal wall jets. Away from the influences of the obstacle's wake, the upwash exhibited increasing decay rates

with decreasing obstacle heights. This behavior asymptotes to the no-obstacle case for small obstacles and to twice the wall jet growth for large obstacles.

A radial wall jet facility was constructed to create a more complex flow configuration. This facility employs a unique design that creates the radial wall jets from source jets below the instrumentation plate. The upwash formed by the collision of these radial wall jets is not influenced by the presence of impinging jets. As in the two-dimensional case, this allows for the systematic investigation of the upwash phenomenon without the additional complications introduced by the impinging jets and re-circulation zone. Preliminary measurements were made in this new configuration.

UNCLASSIFIED

SECURITY CLASSIFICATION OF THIS PAGE

REPORT DOCUMENTATION PAGE

1a. REPORT SECURITY CLASSIFICATION UNCLASSIFIED			1b. RESTRICTIVE MARKINGS	
2a. SECURITY CLASSIFICATION AUTHORITY			3. DISTRIBUTION/AVAILABILITY OF REPORT Approved for Public Release; Distribution Unlimited.	
2b. DECLASSIFICATION/DOWNGRADING SCHEDULE				
4. PERFORMING ORGANIZATION REPORT NUMBER(S)			5. MONITORING ORGANIZATION REPORT NUMBER(S) AFOSR-TR- 84-1197	
6a. NAME OF PERFORMING ORGANIZATION GRUMMAN AEROSPACE CORPORATION		6b. OFFICE SYMBOL (If applicable) AFOSR/NA		7a. NAME OF MONITORING ORGANIZATION AFOSR/NA
6c. ADDRESS (City, State and ZIP Code) BETHPAGE, NY 11714		7b. ADDRESS (City, State and ZIP Code) Bolling AFB, D.C. 20332		
8a. NAME OF FUNDING SPONSORING ORGANIZATION AIR FORCE OFFICE OF SCIENTIFIC RESEARCH		8b. OFFICE SYMBOL (If applicable) AFOSR/NA		9. PROCUREMENT INSTRUMENT IDENTIFICATION NUMBER F49620-82-C-0025
8c. ADDRESS (City, State and ZIP Code) BOLLING AFB, DC 20332		10. SOURCE OF FUNDING NOS.		
		PROGRAM ELEMENT NO. 61102F	PROJECT NO. 2307	TASK NO. A1
11. TITLE (Include Security Classification) AN INVESTIGATION OF TURBULENCE MECHANISMS IN V/STOL UPWASH FLOW FIELDS (UNCLASSIFIED)				
12. PERSONAL AUTHOR(S) GILBERT, BARRY L				
13a. TYPE OF REPORT Annual		13b. TIME COVERED FROM 15 MAR 83 TO 15 JUN 84		14. DATE OF REPORT (Yr., Mo., Day) 1984, August 31
15. PAGE COUNT 56				
16. SUPPLEMENTARY NOTATION <i>study investigated</i>				
17. COSATI CODES			18. SUBJECT TERMS (Continue on reverse if necessary and identify by block number)	
FIELD	GROUP	SUB GR.	JET FOUNTAINS	
			WALL JET COLLISION	
			UPWASH FLOWS	
			V/STOL UPWASH FLOW FIELD	
			TURBULENT MIXING	
19. ABSTRACT (Continue on reverse if necessary and identify by block number) An investigation has been conducted of the two-dimensional upwash region formed by the collision of opposed two-dimensional wall jets. Extensive measurements have been made in the two-dimensional wall jet to establish the starting conditions of the upwash. Evaluation of these measurements has shown classical wall jet behavior, and fully developed mean and turbulence profiles at the collision zone. A unique set of velocity profiles was obtained at seven locations in the upwash. Two components of the velocity were found simultaneously using an X-probe anemometer. By rotating the probe and repeating the profiles, all three velocity components were measured. While mixing layer growth rates were larger than those found in a free two-dimensional jet, these values were less than those reported by previous investigators. The abnormally high turbulence levels reported by other investigators were not found. These data are presented in similarity form. Higher moments and some of the terms in the turbulence kinetic energy equation were also measured. As part of the study of the effect of various				
20. DISTRIBUTION/AVAILABILITY OF ABSTRACT UNCLASSIFIED/UNLIMITED <input checked="" type="checkbox"/> SAME AS RPT <input type="checkbox"/> DTIC USERS <input type="checkbox"/>			21. ABSTRACT SECURITY CLASSIFICATION UNCLASSIFIED	
22a. NAME OF RESPONSIBLE INDIVIDUAL Dr James D Wilson			22b. TELEPHONE NUMBER (Include Area Code) 202/767-4935	22c. OFFICE SYMBOL AFOSR/NA

UNCLASSIFIED

SECURITY CLASSIFICATION OF THIS PAGE

Initial conditions, a series of measurements was taken in the upwash region formed by the collision of unequal wall jets. These are compared to a very simple theory. By choosing a coordinate system aligned with the upwash, these data can be characterized in a pattern similar to the equal wall jet case. Obstacles of various heights were placed at the collision point of equal wall jets. Away from the influences of the obstacle's wake, the upwash exhibited increasing decay rates with decreasing obstacle heights. This behavior asymptotes to the no-obstacle case for small obstacles and to twice the wall jet growth for large obstacles. $h \propto V/\omega$

UNCLASSIFIED

SECURITY CLASSIFICATION OF THIS PAGE

RESEARCH OBJECTIVES

The development of aircraft with vertical/short take-off and landing (V/STOL) capability has led to a requirement for understanding the unique turbulence phenomena encountered in the interaction of lift jets with the ground. When a V/STOL aircraft is in ground effect (IGE), the exhaust from the aircraft lift jets interacts with the ground, producing an upwash flow directed towards the underside of the aircraft. Two characteristics of the upwash flow that make its behavior very difficult to analyze are an apparent, abnormally high turbulence level and a much greater mixing layer (fan width) growth rate compared to other types of turbulent flows (Ref. 1, 2).

This objective of this research is to increase the basic understanding of the turbulent structure in the upwash and to determine those parameters that directly affect the upwash behavior. It is primarily intended to provide a reliable data base for use in predictive computational models. The program is designed to investigate the mechanisms that control turbulence levels, mixing layer spread rate and mean velocity decay rate in the upwash thereby determine the pertinent scaling parameters of the flow.

Although a number of investigations of overall flow in ground effect have been carried out, measurements in these highly unsteady flows are very difficult, and interpretations of these measurements vary widely (Ref. 3-7). The problem is made computationally difficult by the intrinsic three-dimensionality of the upwash. Numerical codes require better definition of the turbulent structure in order to make reliable predictions of the fountain flow and, later, the fountain/aircraft interaction.

Previous investigations have attempted to study the full V/STOL flow field with its full geometric complexity. Some of these have even made measurements with an aircraft planform. These are configuration specific studies that necessarily miss the fundamental flow characteristics. Our approach during most of the first two years was to employ a simple two-dimensional flow configuration. In this configuration, the complex V/STOL upwash flow geometry was simplified. The lifting jet impingement region with the ground has been eliminated. The radially spreading wall jets were replaced by the much simpler two-dimensional wall jets.

During the first (previous) year's effort, the experimental apparatus used to produce a two-dimensional upwash was designed and constructed. After the facility was running and sufficient measurements were obtained to assure two dimensionality and uniformity of the exit profiles, detailed measurements of the wall jet profiles were obtained. These measurements are very important since these two-dimensional wall jets represent the initial flow conditions for the formation region of the upwash. A single wire anemometer was used to measure one component mean and turbulence profiles at six locations in the upwash. These provided a comparison set of data to the relatively small sample of upwash measurements that exist in the current literature. These data appear in the first annual report (Ref. 8).

The second (current) year's effort included the continuation of the upwash measurements. Seven profiles were taken in an equal wall jet upwash using an X-wire hot film anemometer. Repeating these profiles with the probe rotated 90° , we determined all three velocity components. In addition, higher order turbulent moments were measured. Energy spectra and autocorrelation and crosscorrelation measurements, computed with digital fast Fourier transforms, were utilized to determine relevant length scales.

Several experiments were conducted to determine the effect of initial wall jet conditions on the upwash. These were changed in various ways. Using symmetry plates at the position of the collision of equal wall jets, we tested the effects of the stability of the collision point. A study was conducted on the effects of unequal wall jets on the position and turbulence structure in the upwash.

In order to increase the geometric complexity of the flow an experimental apparatus used to produce an upwash from the collision of two radially spreading wall jets was designed and constructed. An unique design was shown to produce a suitably well behaved radial wall jet. This was incorporated in the new facility and tested. Plans for future research include use of this new facility in upwash experiments similar to those described herein for the two-dimensional system.

SIGNIFICANT ACCOMPLISHMENTS

SUMMARY

In this section the significant accomplishments and progress made during the first two years' research effort will be described. The first year's accomplishments were reported in detail in the first annual report (Ref. 8), and many of these results were presented at the AIAA 16th Fluid & Plasma Dynamics Conference, Danvers, MA, July 1983.

In the current year, we provided detailed surveys of the three components of velocity and their statistical moments for several types of wall jet collision regions. We showed effects of unequal jets in a form relatable to the equal-jet case, and investigated effects of dividing plates at the stagnation line and jet initial conditions on the upwash turbulence. During the first year, the test facility was constructed, and a basic set of calibration exit profile data were taken. Wall jet profiles were obtained at 20 locations from the jet exit to the facility centerline. These surveys showed the rapid development of the mean and turbulence similarity profiles. They also exhibited the well established mixing layer growth rate and mean velocity decay rate that characterize wall jets. Careful measurements were made at six heights in the upwash. The expected abnormally high mixing layer growth rate was found in the two-dimensional upwash flow. However, the turbulent intensity was of the same order as is found in ordinary two-dimensional free jets. Our set of carefully generated data from a well defined two-dimensional source shows symmetry of the turbulence energy profiles in the upwash, data not previously reported. These baseline upwash data show mean velocity decay and spread rate trends required by conservation considerations, trends which have eluded some earlier investigators. These X-hot film probe measurements have shown, for the first time, the cross component mean velocity in the upwash. In addition, the turbulence profiles for both components were obtained. Finally, one component of the Reynolds stress was measured. As a sign of the accuracy of the measurement technique, these cross component data show remarkable symmetry.

During the second year, the baseline data set was repeated using X-hot film probes to measure three components of velocity. Data were taken at seven

locations in the upwash formed by equal wall jet collisions. Component measurements were taken in the free stream and both cross stream directions, which included mean, fluctuation and higher moments found in the turbulent kinetic energy equation. In addition, microscales and integral scales were calculated from the time series using a fast Fourier transform to compute the energy spectra and the inverse transform to compute the autocorrelation and crosscorrelations. Another task was an investigation of the effects of the wall jet initial conditions, particularly along the stagnation line, on the upwash turbulence characteristics (Ref. 6, 9, 10). The location of a small object on the stagnation line serves to stabilize the upwash. The object will also isolate the turbulent structures in each wall jet from each other during the critical turning phase. Our experiments employed wall jets flowing into "symmetry" planes. After a baseline set of data was obtained, the height of the dividing "symmetry" plane was successively shortened until the real two jet upwash jet flow was simulated. As part of this task, unequal wall jets were used to form an upwash. Basic turbulence characteristics were measured in these flows for five different initial pressure ratio levels at four heights in the upwash.

The final task was the design and construction of the next more complicated flow configuration. In this configuration, the upwash is formed by the collision of radially spreading wall jets. In order to assure that there would be no influence with the upwash development due to the presence of the source jet, a unique design was employed. The source of the radial jet is from below the instrumentation plate. The axisymmetric radial wall jet is formed by the collision of the circular source jet and a closely spaced deflector plate. This produces a suitable radial wall jet for the next phase of the study.

WALL JET

The wind tunnel facility designed and constructed for most of the first two years' effort is diagrammed in Fig. 1, and the test section is shown in Fig. 2. It is described in the first annual report (Ref. 8). To facilitate understanding and comparing the data, a coordinate system was chosen that allows the X direction to be the mean direction of the largest velocity component. That is, X tracks some centerline streamline and Y is always perpendicular to it. This results in a 90° rotation of X from the wall jet to

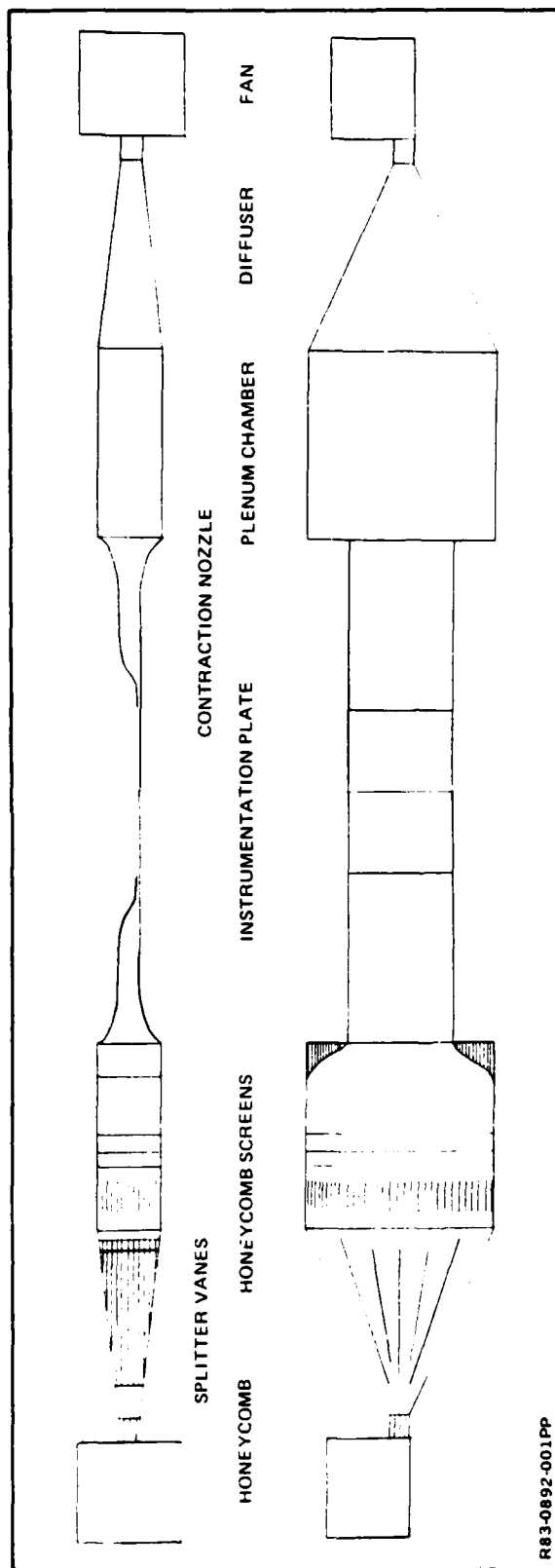


Fig. 1 Diagram of Two-dimensional Jet Upwash Facility



Fig. 2 Photograph of Two-dimensional Jet Upwash Facility

the upwash as shown in Fig. 3. For clarity, wall jet parameters are indicated with the subscript 'w'. U and u' are the mean and rms fluctuation components in the X direction. V and v' are the components in the Y direction.

Figure 4 shows hot film anemometry measurements of a typical exit plane velocity profile taken vertically across the nozzle exit and includes the entrained flow velocity over the top of the nozzle. If the boundary layer is disregarded, the mean velocity is uniform to 0.75%, controllable to 67 m/sec, with turbulent intensities u'/U of about 0.6%. The single jet external entrainment velocity increases from about 6.6% of the mean exit velocity to 9.7% when both wall jets are used to form an upwash. The instrumentation plate is 84 cm long (nozzle to nozzle).

Wall jet mean and turbulence profiles were taken at 20 locations from the jet exit nozzle to the instrumentation plate centerline. These profiles were made at equal distances along the plate in increments of approximately two nozzle heights. Each profile contains 24 data points. The data acquisition and positioning of the single element hot film probe were accomplished under the total control of the automatic digital data system.

A plot of the wall jet growth rate as characterized by the half velocity height vs the distance downstream is given in Fig. 5a. A linear least squares curve fit of the data from stations 6 through 20 ($X_w/D_w > 10$) gives a growth rate of 0.0728. This is exactly the growth rate established as the "correct" value for self-preserved two-dimensional wall jets on plane surfaces at the 1980-81 AFOSR-HTTM Stanford Conference (Ref. 11) of 0.073 ± 0.002 . The first five stations were eliminated from the curve fit because they are in the development region. Figure 5b shows the linear decay of the maximum velocity squared vs distance. This relationship is required by conservation of momentum considerations. The data were normalized by the characteristic half height dimension and the 10 alternate profiles were plotted. Figure 6 shows that the mean velocity similarity exists as early as $X_w/D_w = 10$, much sooner than the 50 slot heights quoted at Stanford. Figure 7 shows the 10 alternate turbulence profiles normalized by the half velocity width. These show similarity at X_w/D_w about 20.

The wall jet characteristics at the centerline of the collision zone may be determined. The centerline is at $X_w/D_w = 42$. The wall jet parameters when no collision occurs should be used to normalize upwash data in a manner

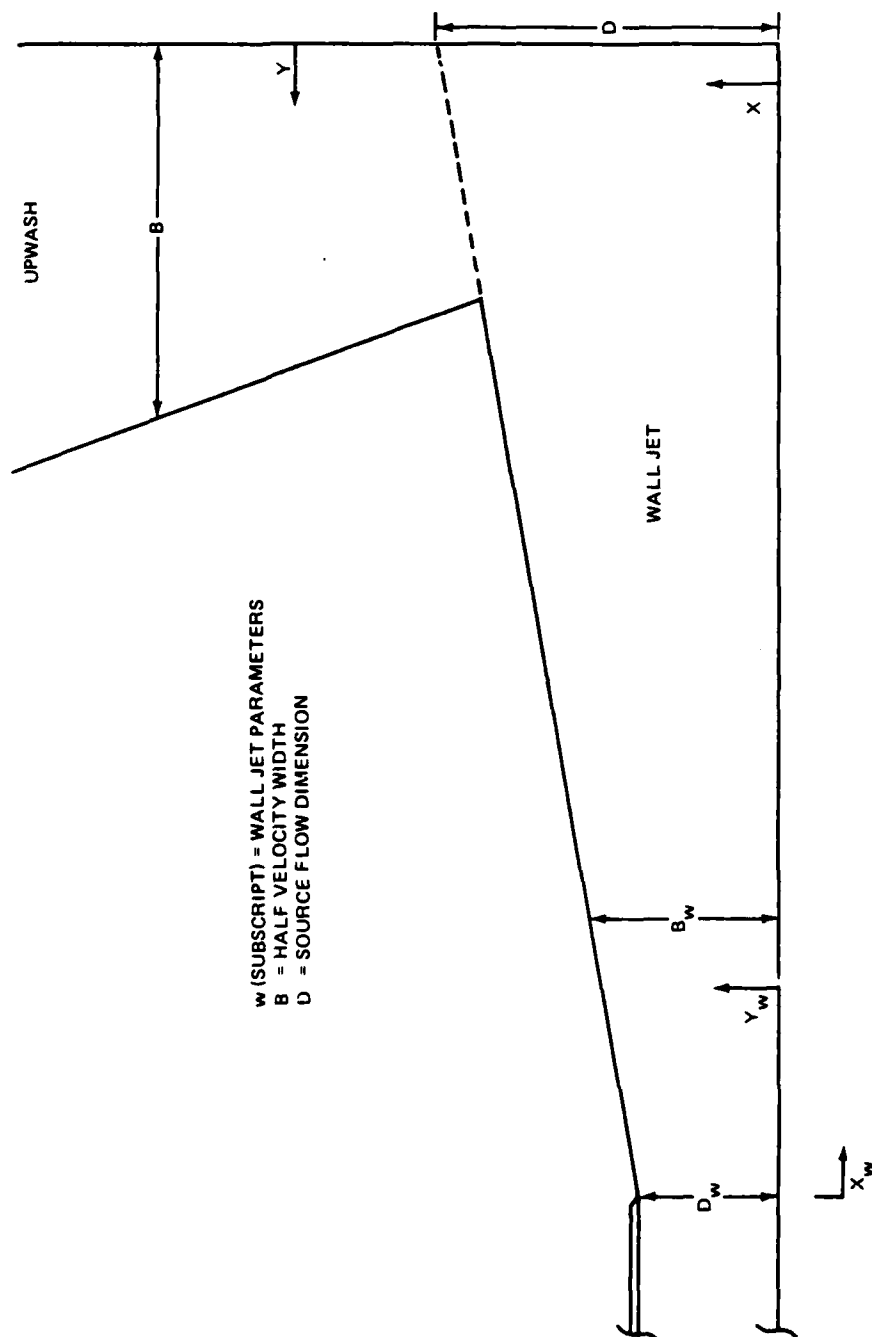
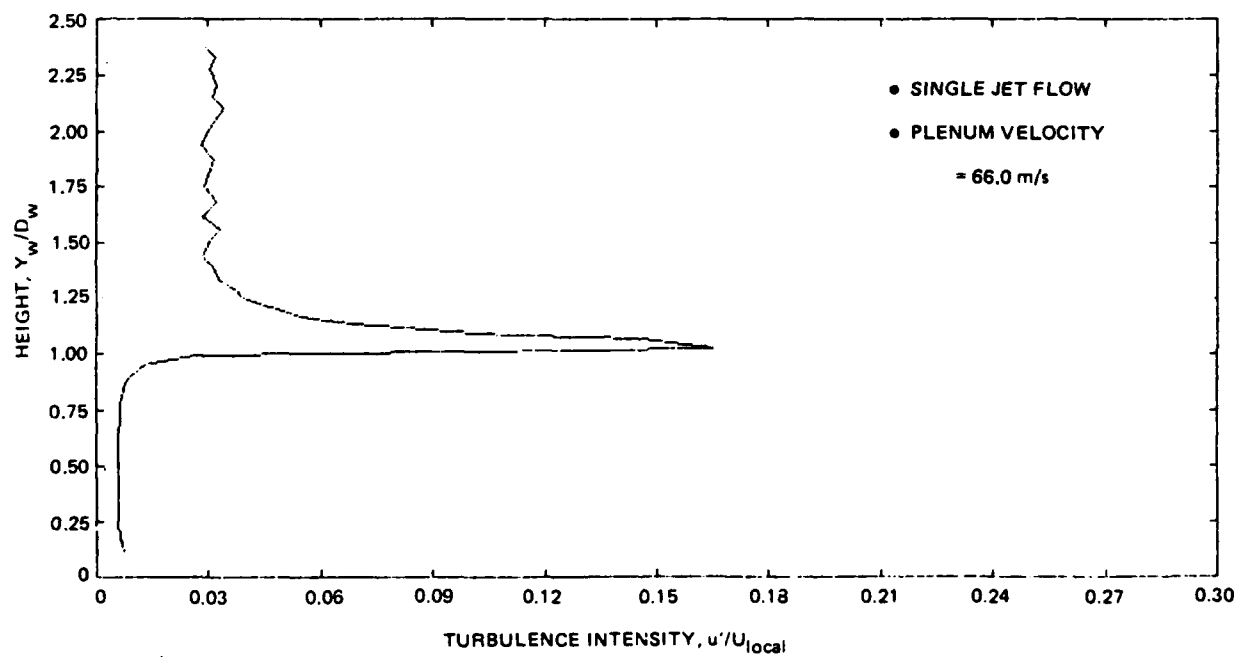
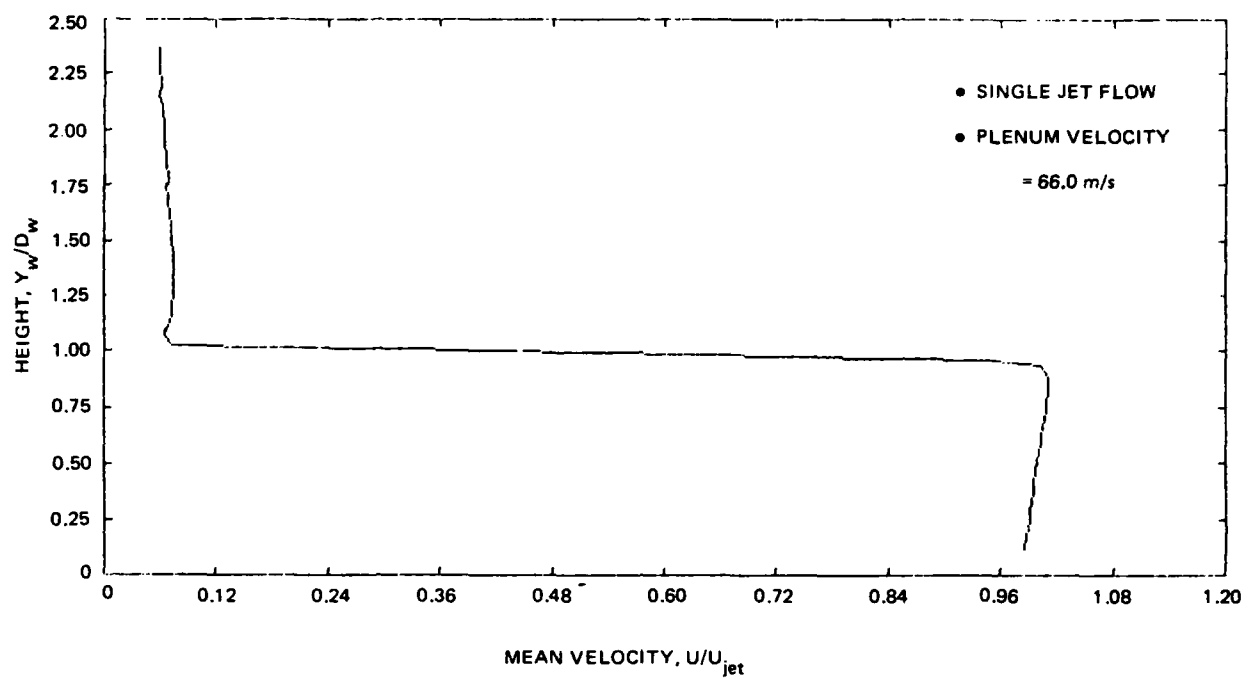


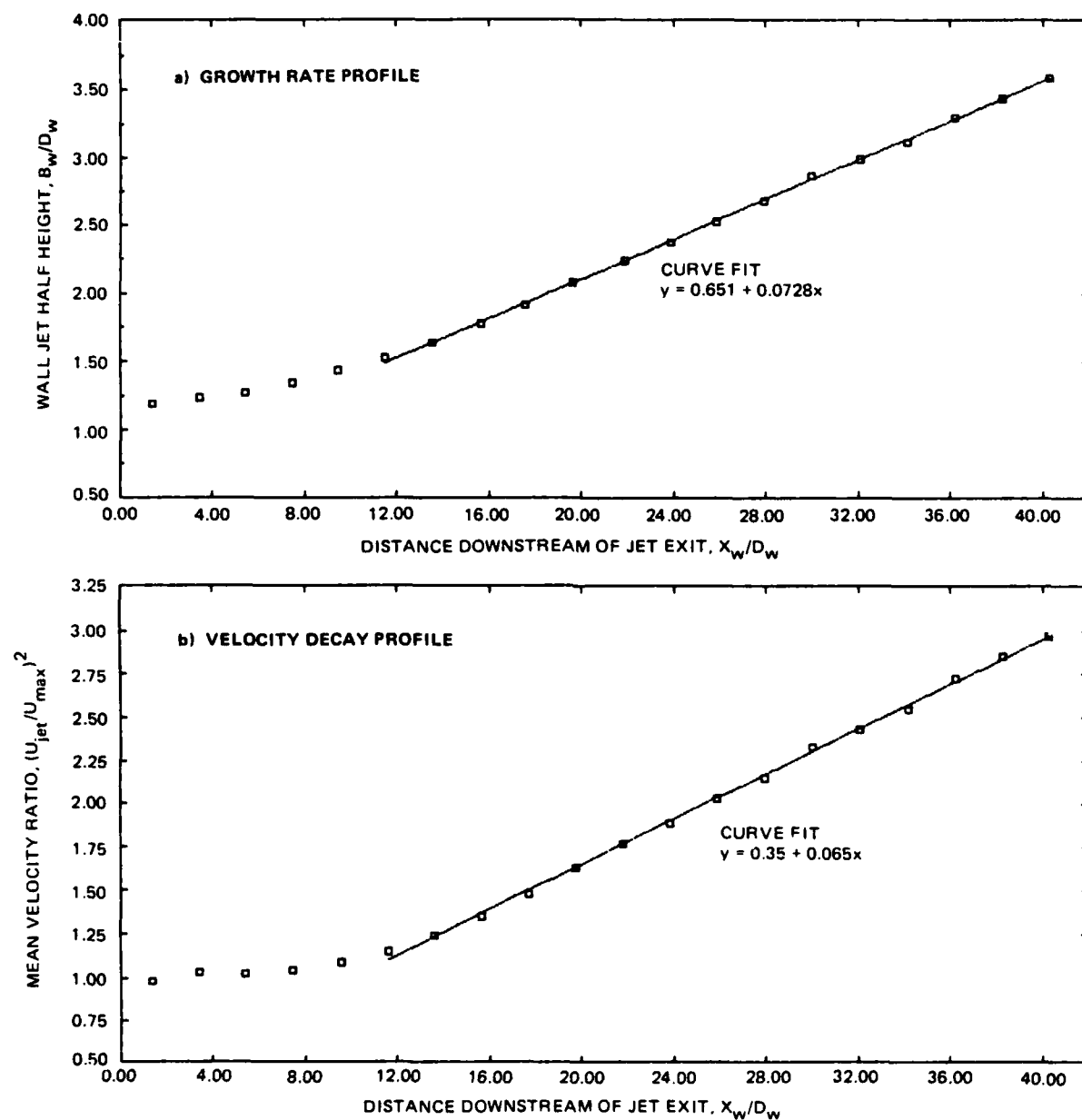
Fig. 3 Coordinate System Nomenclature Conversion

R83-0892-003PP



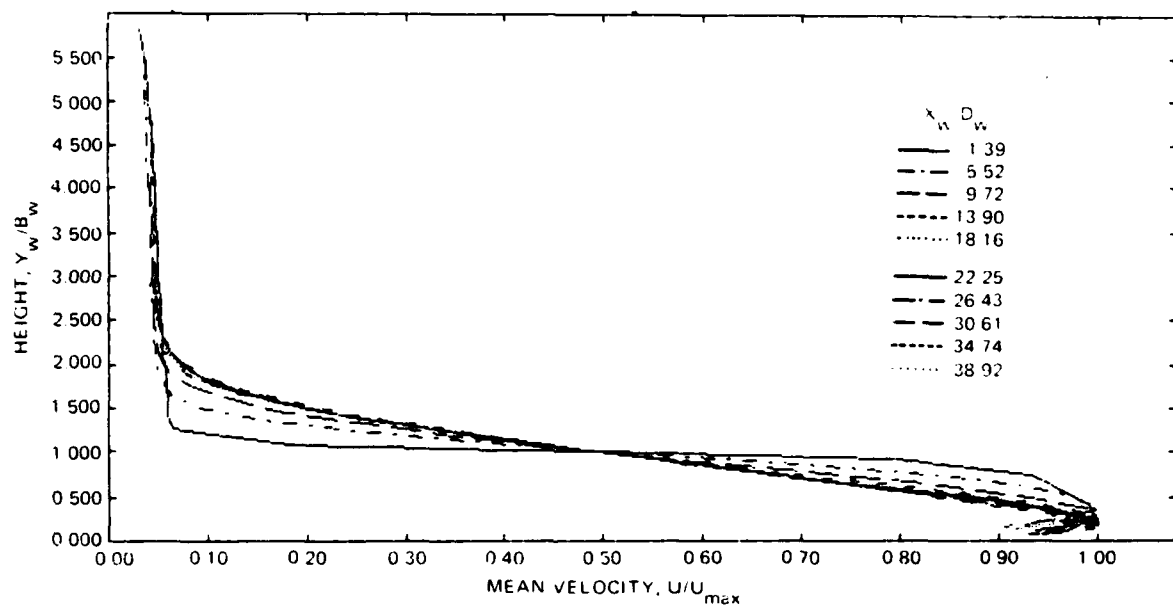
R83-0892-004PP

Fig. 4 Typical Jet Exit Velocity Profiles



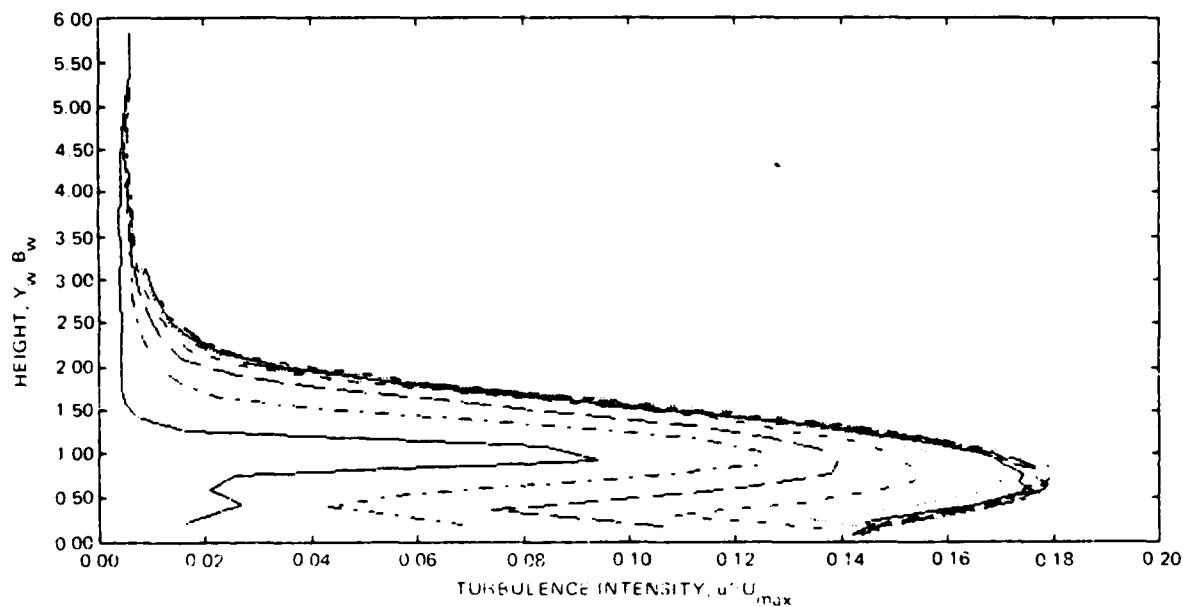
R83-0892-007PP

Fig. 5 Two-dimensional Wall Jet Characteristics



R83-0892-008PP

Fig. 6 Wall Jet Mean Velocity Profiles in Similarity Form



R83-0892-010PP

Fig. 7 Wall Jet Turbulence Intensity Profiles in Similarity Form (See Fig. 6 For Symbol Key)

similar to using the wall jet nozzle height as an initial characteristic dimension. At the centerline, the wall jet half height is $B_w/D_w = 3.702 = D$ for the upwash and $U_{max}/U_{jet} = 0.571$ at the centerline.

EQUAL JET UPWASH

The upwash formed from the collision of two equal wall jets was probed extensively. The basic set of measurements was taken at seven heights ($X/D = 2, 3, 4, 5, 6, 8$ and 1). The last of these is separate since, as will be shown, at $X/D = 1$ the flow is still turning and is not yet fully in the upwash direction. This should be expected from the fact that D is the wall jet half velocity height, and therefore significant flow along the wall is above this point. These equal wall jet data were taken repeatedly and always produced the same results.

The data were taken using an X-wire hot film anemometer probe. An X-probe measures two components of the velocity simultaneously. After measuring the mean flow and one cross flow component, rotating the probe 90° about its axis provides a repeat of the mean flow and the other cross flow component. The data acquisition process was controlled by a digital computer. The program positioned the probe, acquired the data, performed the appropriate processing, and stored the processed raw data on disk. The profile information is constructed from 60 points, each 5.9 mm apart. That is, initially $y/D = 0.16$. Of course, as one continues up the upwash, the characteristic dimension gets larger and the relative data spacing gets smaller. At each point, 32768 data pairs were taken in blocks of 4096 representing a time series of 13.4 seconds. There are two forms of the data analysis program. One does a complete turbulence analysis and the other only computes means, turbulence energy, and one component Reynolds stress. The complete program, in addition, computes third and fourth moments, autocorrelations and crosscorrelations, Taylor microscales and integral scales. These allow calculation of various terms in the turbulent kinetic energy equation, and intermittency. The length scales are calculated by computing the turbulence energy spectra from the time series by using fast Fourier transforms and then computing the correlation using the inverse transform. The Taylor scales were also computed from the derivative of the time series for comparison. Because taking derivatives inherently adds noise, these values are not as reliable as those obtained from the correlation

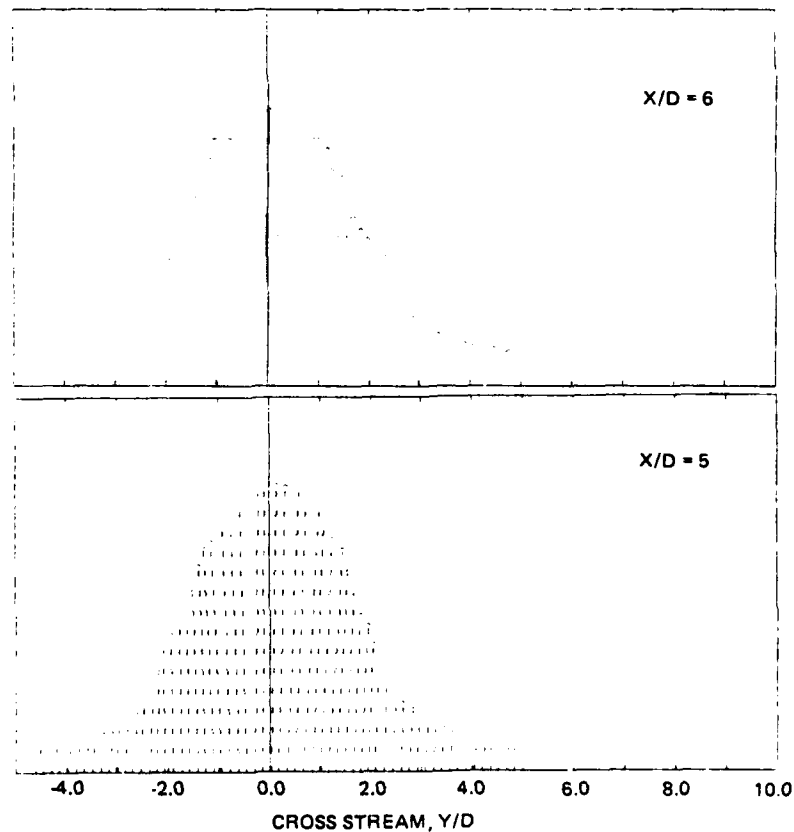
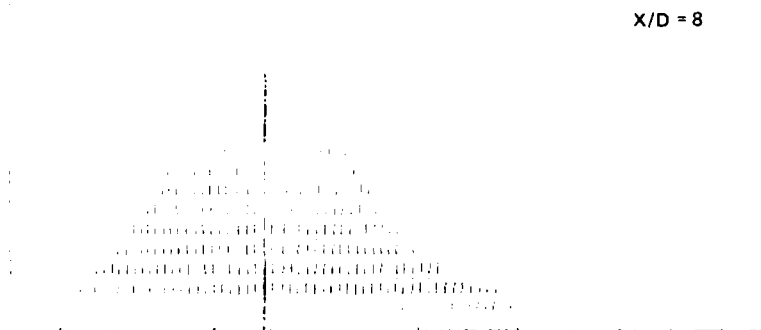
except at the centerline, where the intermittency is one and the values agreed well.

The upwash vectors are shown in Fig. 8. The residual velocities in the tails are similar to other studies (Ref. 3-7). The flow in the tails is the entrainment flow, which has been verified by smoke flow visualization studies. The mean velocity profiles are symmetric, and, beyond $X/D = 2$, the turbulence profiles have symmetric peaks. Kotansky does not give these turbulent profile data (Ref. 5); Witze (Ref. 4) and Foley (Ref. 6) show only one-sided turbulence measurements, that is, they do not show the symmetric data; only Kind and Suthanthiran (Ref. 3) show the complete profiles and their data are not symmetric.

The mean velocity profiles in the upwash direction were curve fit with a least square curve of the form $U = A + C \exp [-(Y - Y_0)^2/2S^2]$. This curve fit gives the symmetry coordinate y_0 , the maximum velocity $(A+C)$, and the standard deviation S . Using the generally accepted definition of half velocity width, $B(U = U_{\max}/2) = 1.177 S$. It should be emphasized that our technique is far superior to the usual determination of half width. That procedure usually entails finding U_{\max} and interpolating between data points to determine B . The latter method suffers severely from scatter in the data at both U_{\max} and particularly at the half velocity point. Also, it rarely gives symmetric half velocity positions. A least squares curve fit avoids these problems. The results for the half velocity growth so defined are shown in Fig. 9a.

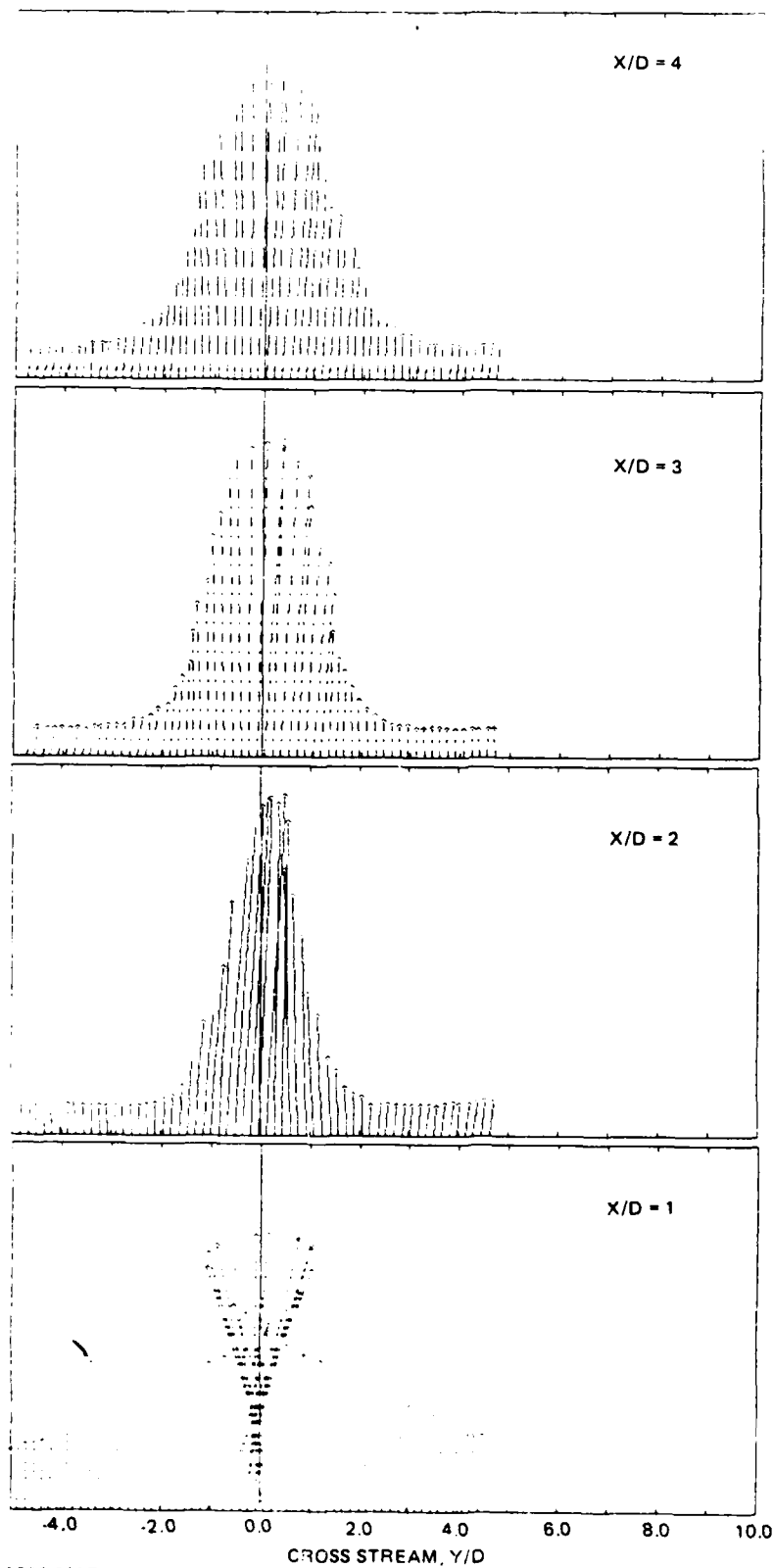
The growth rate is about 0.23, which doesn't agree with previously reported results (Ref. 3-7), but values between 0.22 and 0.23 were repeatedly obtained in these experiments. This value is more than twice the free jet value. A closer look at these other data shows inconsistency, and, in some cases, plotted data disagree with written statements. The proper mean velocity decay characteristic is shown in Fig. 9b for X/D greater than 2.0. This is the form for the mean velocity decay required by conservation of axial momentum in the upwash, a characteristic not usually found by others. Between $X/D = 1.0$ and 2.0, the mean velocity actually increases and the mixing width decreases correspondingly. This is a strong indication that the extent of the collision zone is of the order of 2.0 D .

The mean velocity profiles at six heights are shown in Fig. 10. The profiles have been shifted to their symmetry point and normalized by the local



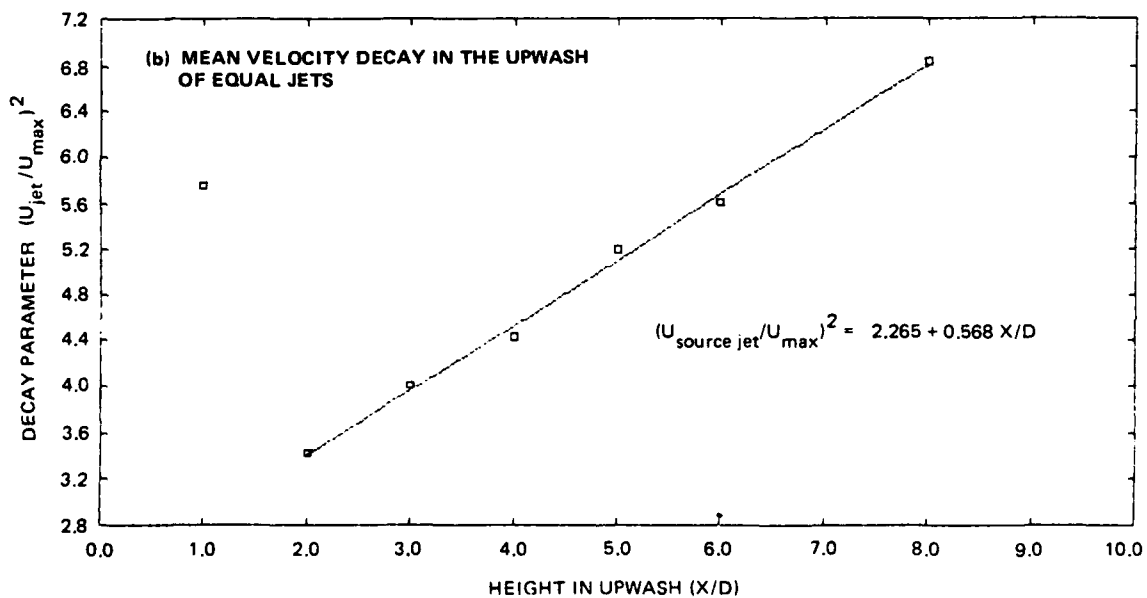
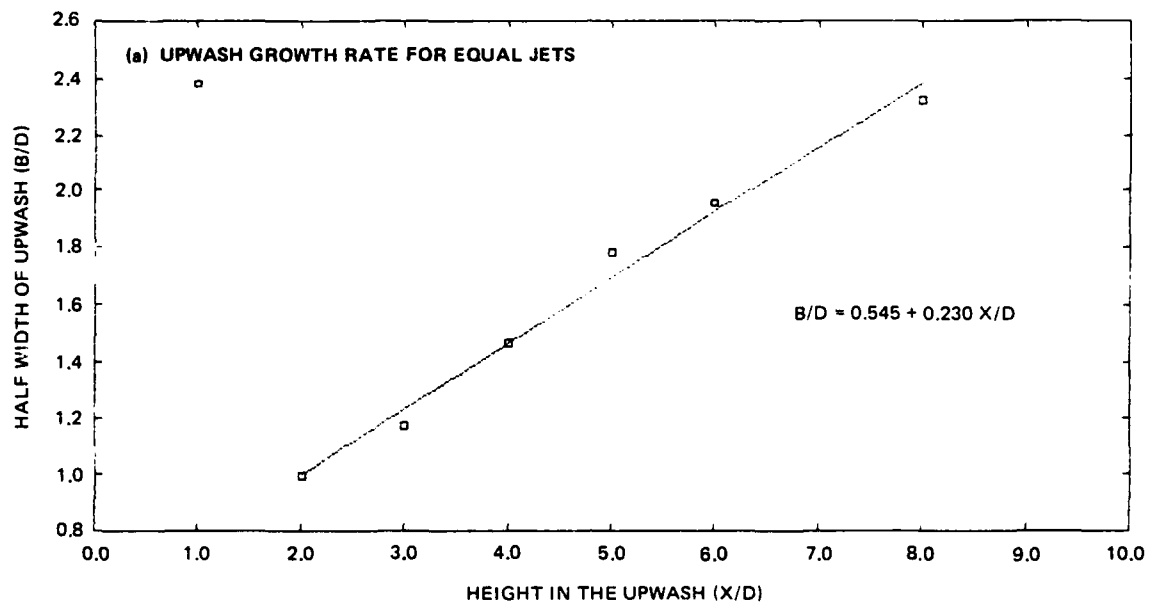
1335-001D

Fig. 8 Upwash Flow Field Vectors for Equal Wall Jets at Seven Heights (Sht. 1 of 2)



1335-001D

Fig. 8 Upwash Flow Field Vectors for Equal Wall Jets at Seven Heights (Sht. 2 of 2)



1335-002D

Fig. 9 Spread Rate and Mean Velocity Decay in a Two-dimensional Upwash

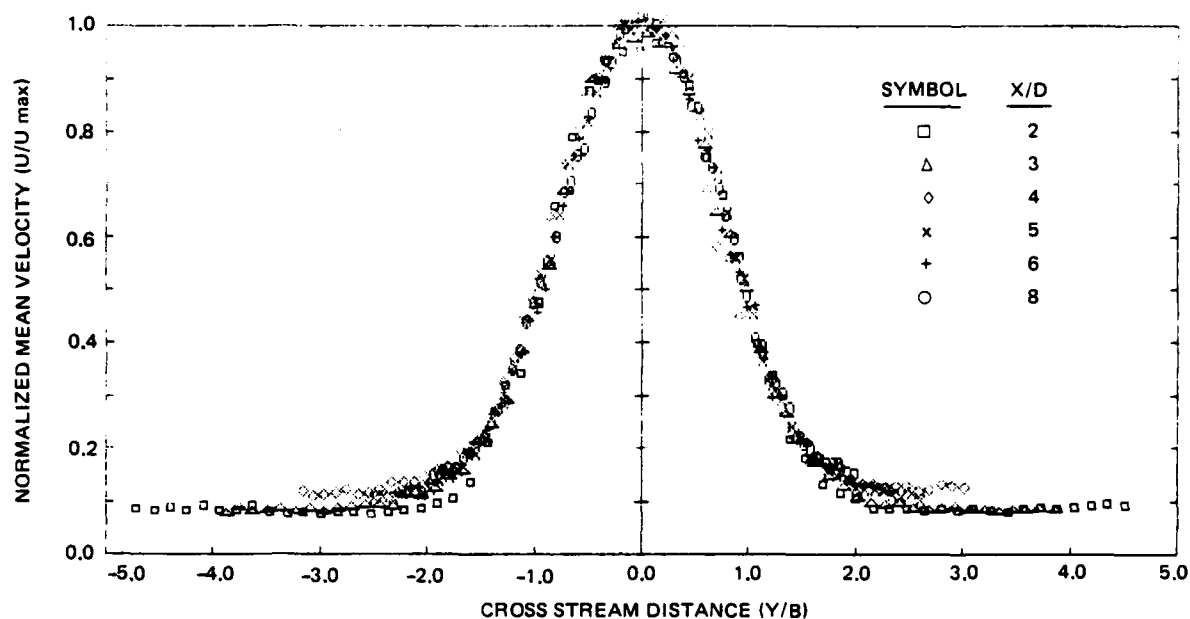
half velocity width and local maximum mean velocity as determined by the curve fit. These similarity profiles for X/D greater than 2.0 may be expressed as

$$\frac{U}{U_{\max}} = \exp \{-0.693 n^2\} \text{ where } n = Y/B.$$

The component turbulence energy does not reach similarity as rapidly. The component in the mean flow direction is shown in Fig. 11. Similarity is reached at about $X/D = 5$, which is much faster than usually found in 2-D free jets. This may be due to the fact that there is no core region that needs to decay before the similarity jet can form. These profiles are normalized in a manner similar to the mean profiles. The magnitude and form of these profiles are exactly those expected to be found in a two-dimensional plane jet. The components in the other two cross stream directions, obtained by rotating the probe, are shown in Fig. 12 and 13. Again these show the expected form and values. Figure 14 shows the total turbulent kinetic energy profile at six heights, normalized as before. The total energy q^2 reaches similarity quite rapidly, showing that the slower development of the individual components is really due to a redistribution of turbulence among the various components as they approach local isotropy. Figure 15 shows the ratio w'^2/v'^2 . Throughout most of the center region, between $Y/B = -1$ to $+1$, this ratio is approximately 0.85. Therefore, calculations of q^2 when w data were not taken will be defined as $q^2 = (u'^2 + 1.85 v'^2)$.

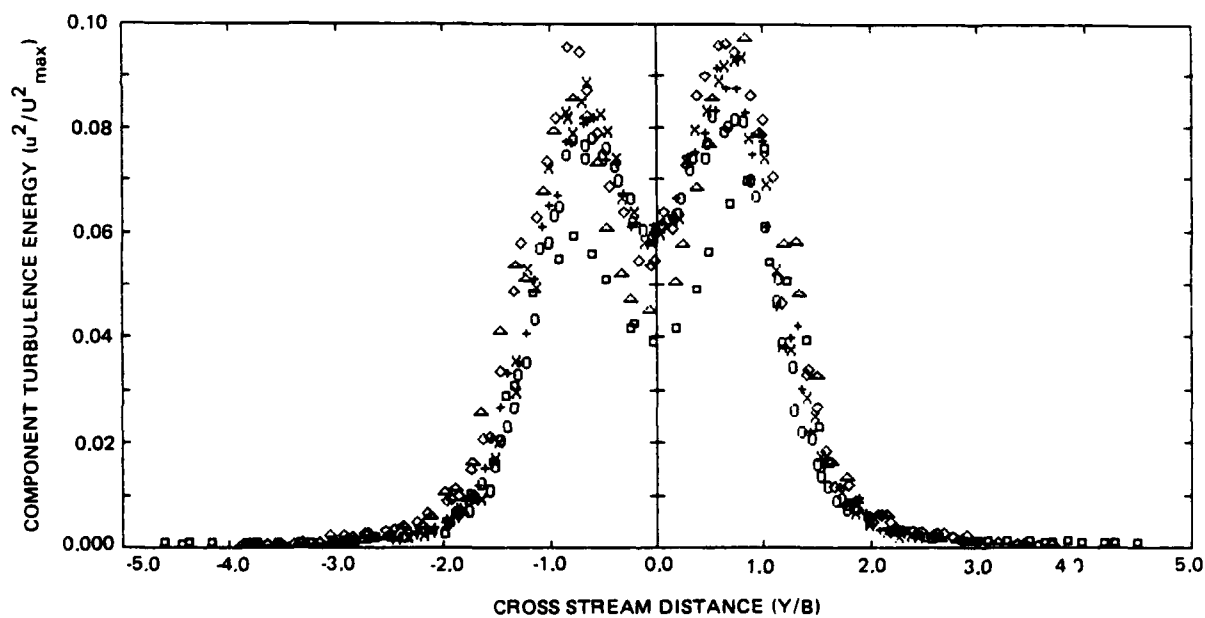
Examination of the component turbulence energy and total kinetic energy levels found in the upwash shows these values to be exactly the same as those found in ordinary two-dimensional free jet flows. This is contrary to statements made by Foley (Ref. 6) and Witze (Ref. 4) that the turbulence intensity is a factor of three greater than the free jet case. However, examination of their data indicates ordinary levels. Only Kind and Suthanthiran (Ref. 3) show factors of three. Kotansky (Ref. 5) shows no turbulence data at all.

Figure 16 shows one component of the Reynolds stress, uv . Across the center region, the Reynolds stress profiles are anti-symmetric about the centerline passing through zero and have the same magnitude on either side. Since Reynolds stress measurements are particularly sensitive to measurement techniques, these plots are a good indication of the precision of the entire experiment. The form and magnitude are again exactly those expected in a two-dimensional jet.



1335-003D

Fig. 10 Mean Velocity Profiles for Equal Wall Jet Upwash at Six Heights in Similarity Form



1335-004D

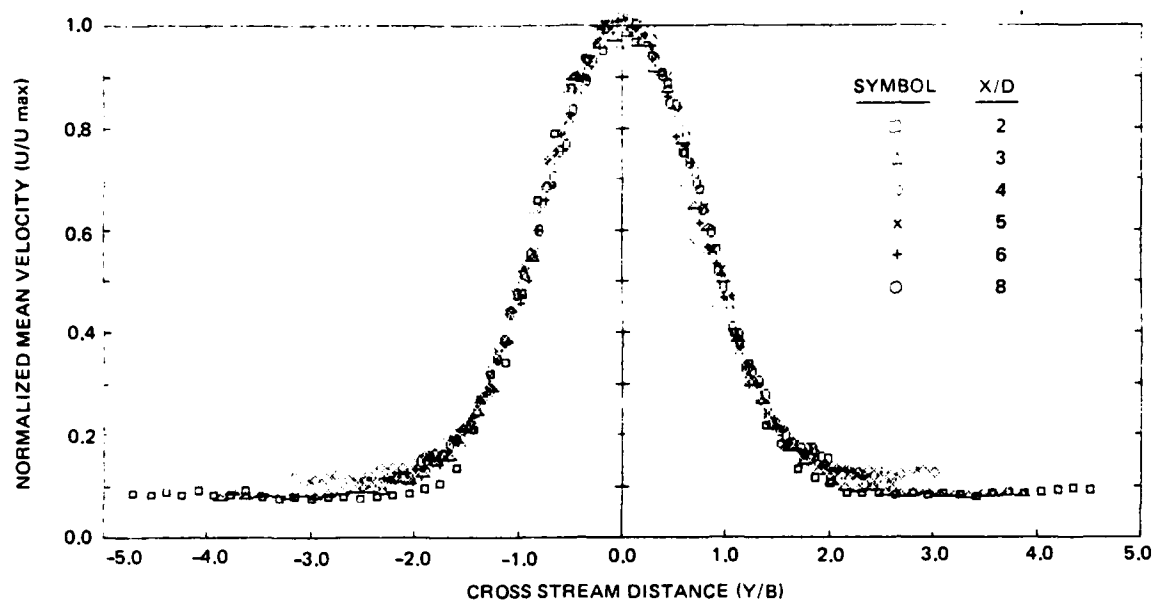
Fig. 11 Component Turbulence Energy in the Mean Flow Direction at Six Heights
(See Fig. 10 for Symbol Key)

half velocity width and local maximum mean velocity as determined by the curve fit. These similarity profiles for X/D greater than 2.0 may be expressed as $\frac{U}{U_{\max}} = \exp -0.693 \left(\frac{Y}{B}\right)^2$ where $\frac{Y}{B} = Y/B$.

The component turbulence energy does not reach similarity as rapidly. The component in the mean flow direction is shown in Fig. 11. Similarity is reached at about $X/D = 5$, which is much faster than usually found in 2-D free jets. This may be due to the fact that there is no core region that needs to decay before the similarity jet can form. These profiles are normalized in a manner similar to the mean profiles. The magnitude and form of these profiles are exactly those expected to be found in a two-dimensional plane jet. The components in the other two cross stream directions, obtained by rotating the probe, are shown in Fig. 12 and 13. Again these show the expected form and values. Figure 14 shows the total turbulent kinetic energy profile at six heights, normalized as before. The total energy q^2 reaches similarity quite rapidly, showing that the slower development of the individual components is really due to a redistribution of turbulence among the various components as they approach local isotropy. Figure 15 shows the ratio w'^2/v'^2 . Throughout most of the center region, between $Y/B = -1$ to $+1$, this ratio is approximately 0.85. Therefore, calculations of q^2 when w data were not taken will be defined as $q^2 = (u'^2 + 1.85 v'^2)$.

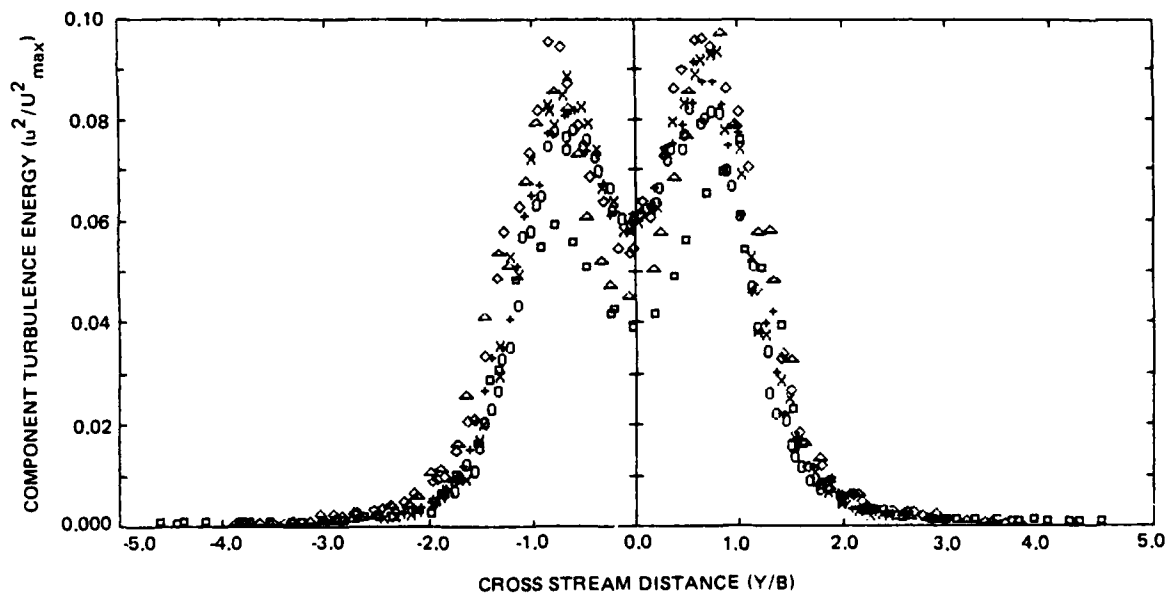
Examination of the component turbulence energy and total kinetic energy levels found in the upwash shows these values to be exactly the same as those found in ordinary two-dimensional free jet flows. This is contrary to statements made by Foley (Ref. 6) and Witze (Ref. 4) that the turbulence intensity is a factor of three greater than the free jet case. However, examination of their data indicates ordinary levels. Only Kind and Suthanthiran (Ref. 3) show factors of three. Kotansky (Ref. 5) shows no turbulence data at all.

Figure 16 shows one component of the Reynolds stress, uv . Across the center region, the Reynolds stress profiles are anti-symmetric about the centerline passing through zero and have the same magnitude on either side. Since Reynolds stress measurements are particularly sensitive to measurement techniques, these plots are a good indication of the precision of the entire experiment. The form and magnitude are again exactly those expected in a two-dimensional jet.



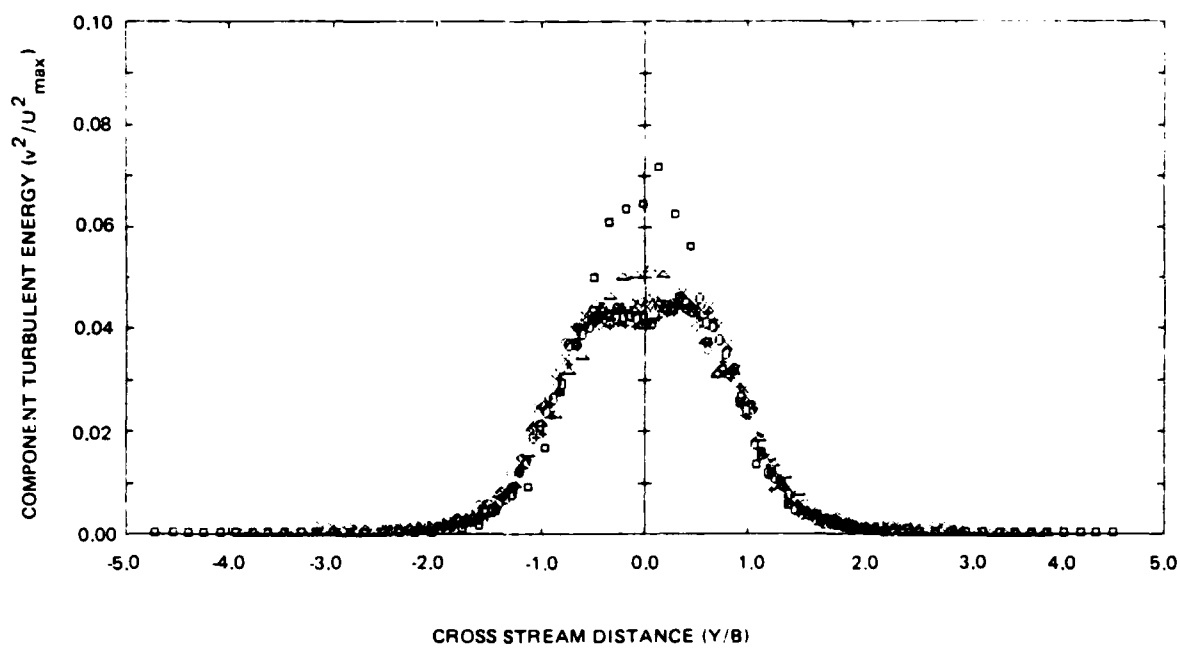
1335-003D

Fig. 10 Mean Velocity Profiles for Equal Wall Jet Upwash at Six Heights in Similarity Form



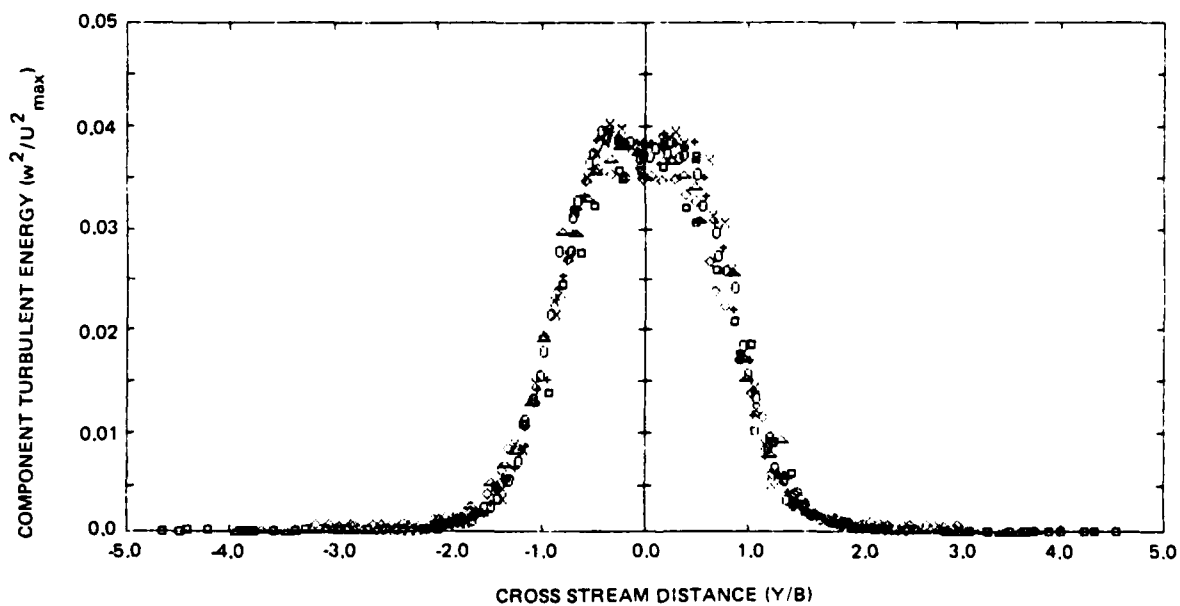
1335-004D

Fig. 11 Component Turbulence Energy in the Mean Flow Direction at Six Heights
(See Fig. 10 for Symbol Key)



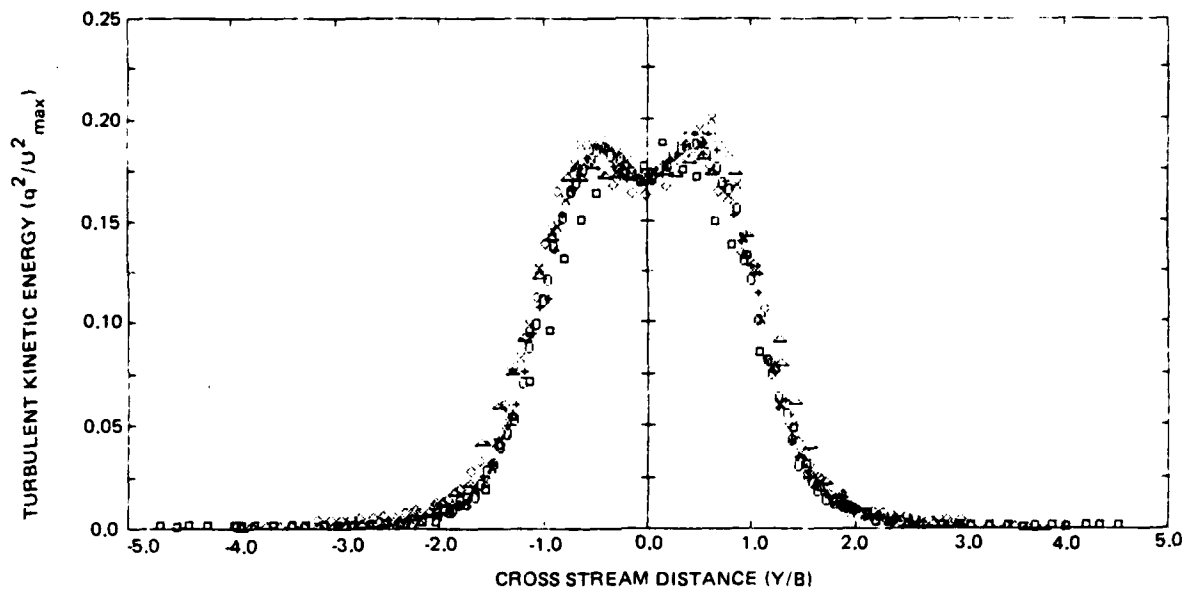
1335-005D

Fig. 12 Component Turbulence Energy in the Cross Flow Direction at Six Heights
(See Fig. 10 for Symbol Key)



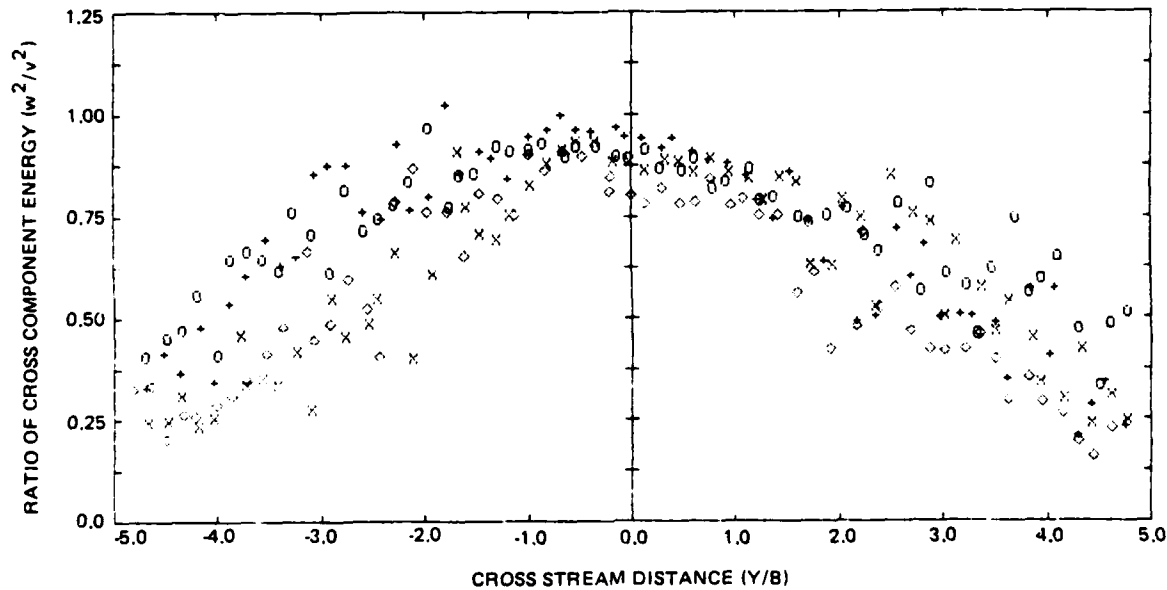
1335-006C

Fig. 13 Component Turbulence Energy in the Third Orthogonal Direction at Six Heights
(See Fig. 10 for Symbol Key)



1335-007D

Fig. 14 Total Turbulence Kinetic Energy in an Equal Wall Jet Upwash at Six Heights
(See Fig. 10 for Symbol Key)



1335-008D

Fig. 15 Ratio of the Cross Component Turbulence Energy
(See Fig. 10 for Symbol Key)

In addition to growth rate, another departure from free jet characteristics is found in the intermittency. Figure 17 shows the normalized intermittency. The intermittency is determined by the flatness factor normalized by the centerline value. An intermittency factor of one indicates fully turbulent flow. The form of these curves is the expected normal distribution. However, in all free shear flows, the ratio of the intermittency half width to mean velocity half width is two (Ref. 12). Here, it is one. Remember, all of the profiles shown have been normalized by local mean velocity half widths. So, while the form looks absolutely correct, the widths of the profiles are about twice the free jet widths. Because of the method of normalization, this means that the intermittency profile is really very similar to the free jet profile. These are shown as the same curve on the diagram Fig. 18. Figure 18 also shows the relationship of the turbulence and mean profiles in free and upwash flows. The relative mixing layer growth rates are represented at the bottom of the figure. Because the upwash intermittency profile does not have a flat region at the centerline, the non-turbulent flow outside the upwash is penetrating nearly to the centerline. That is, the mixing layer must have a penetration length scale nearly equal to the half velocity width. This is apparent from the length scale profiles shown in Fig. 19. These integral scale lengths were obtained by integrating the area under the autocorrelation curve to the point of the first zero crossing. This length scale is representative of the size of the large scale motions responsible for mixing. Through the center region, it is seen that these are a significant percent of the local mean velocity half width. These values are much larger than those found in a free jet flow, again by a factor of two!

The turbulent microscale is shown in Fig. 20. This scale, representative of the energy dissipation length, was calculated in two different ways. It was directly calculated from the derivative of the time series. This method suffers from the inherent noise increase by differentiation. In addition, due to the intermittency away from the centerline, the average values at a point are prejudged towards lower values. The second method computes the scale from the second derivative of the autocorrelation function at the origin. At the centerline, these two methods give good agreement. Figure 20 utilizes the second method. The values are nearly constant across the mixing layer as assumed in some mixing length turbulence models. The values are unusually

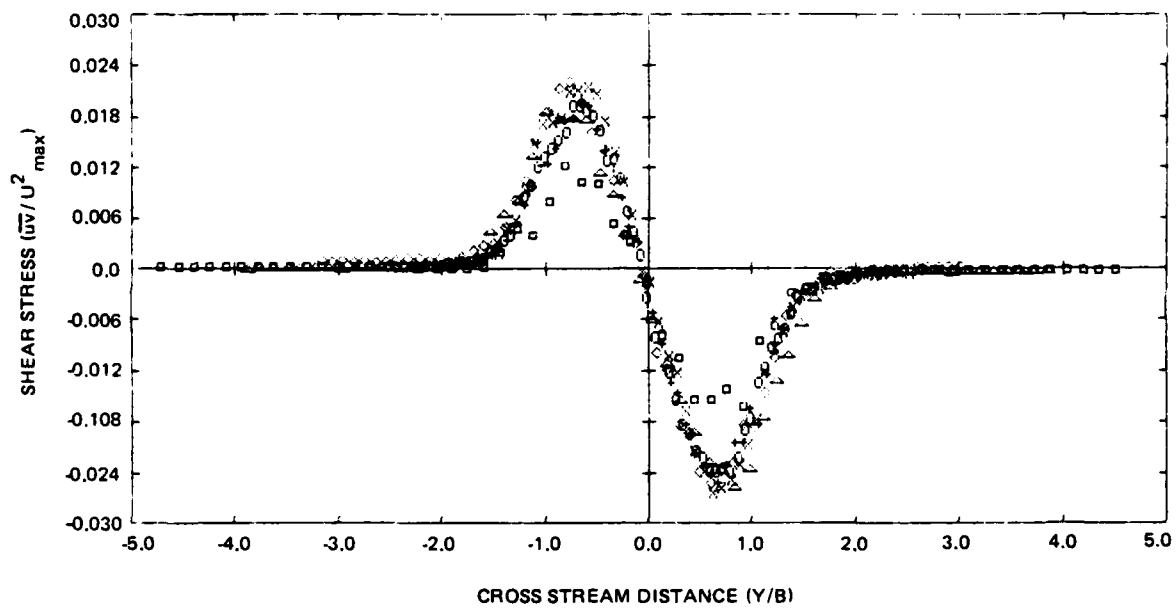


Fig. 16 Shear Stress Component in an Upwash at Six Heights (See Fig. 10 for Symbol Key)

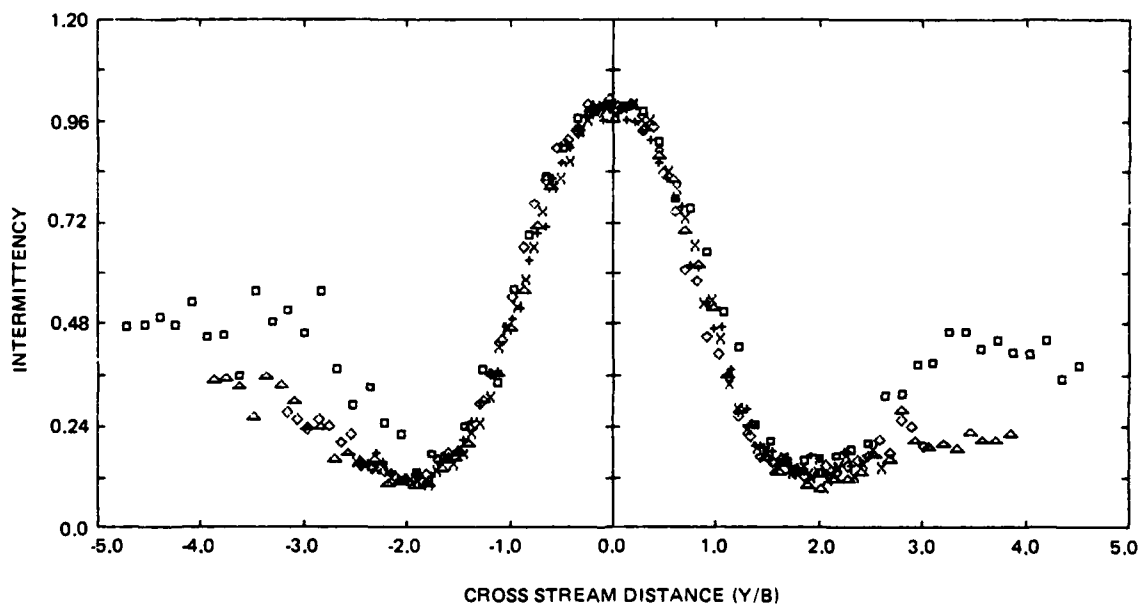
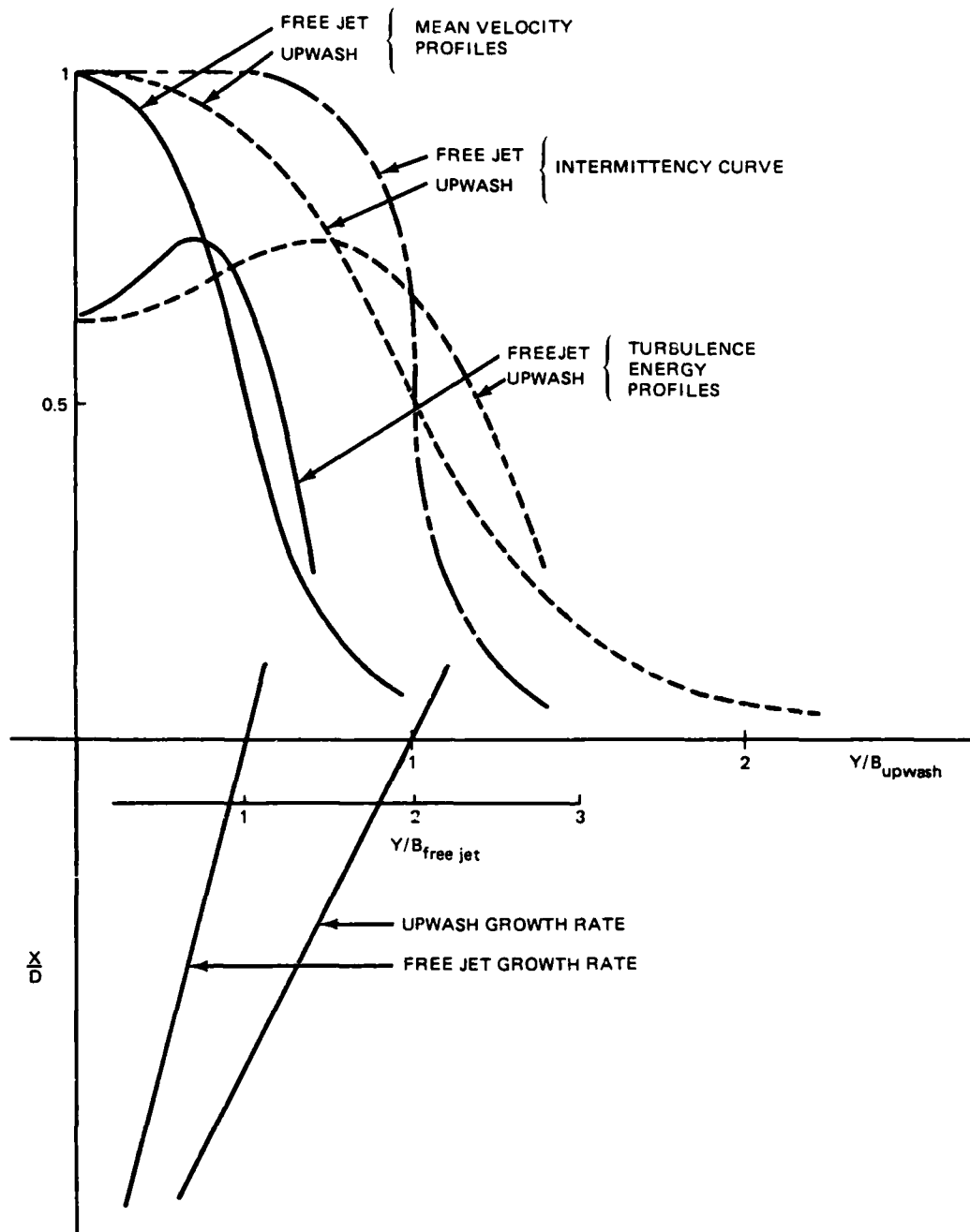
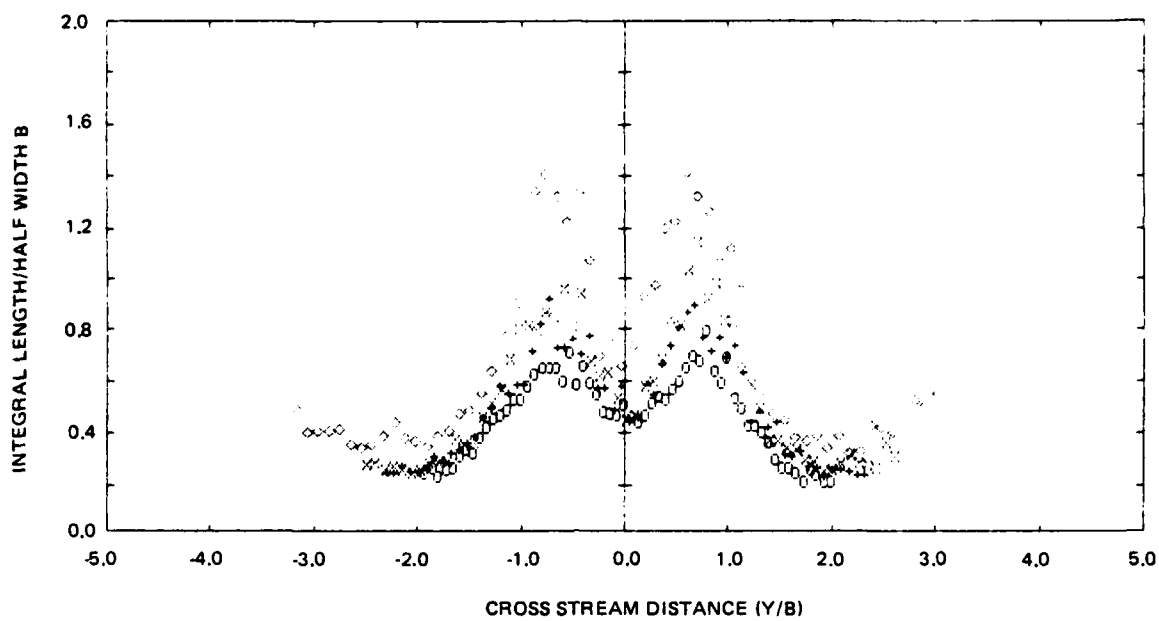


Fig. 17 Intermittency Profiles in an Equal Jet Upwash (See Fig. 10 for Symbol Key)



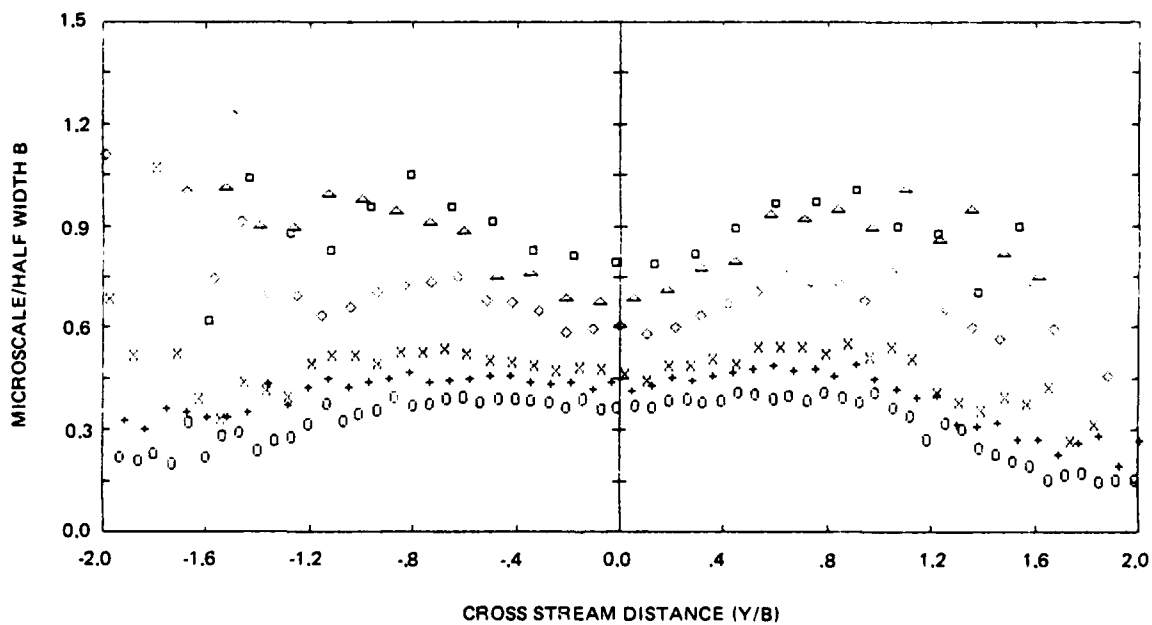
1335-011D

Fig. 18 Comparison of Mean and Turbulence Profiles for a Free 2-D Jet with a 2-D Upwash



1335-012D

Fig. 19 Integral Scale Lengths Across 2-D Upwash (See Fig. 10 for Symbol Key)



1335-013D

Fig. 20 Taylor Micro-scale Lengths Across 2-D Upwash (See Fig. 10 for Symbol Key)

large indicating greater than normal turbulence dissipation consistent with the increased mixing rate.

UNEQUAL WALL JETS

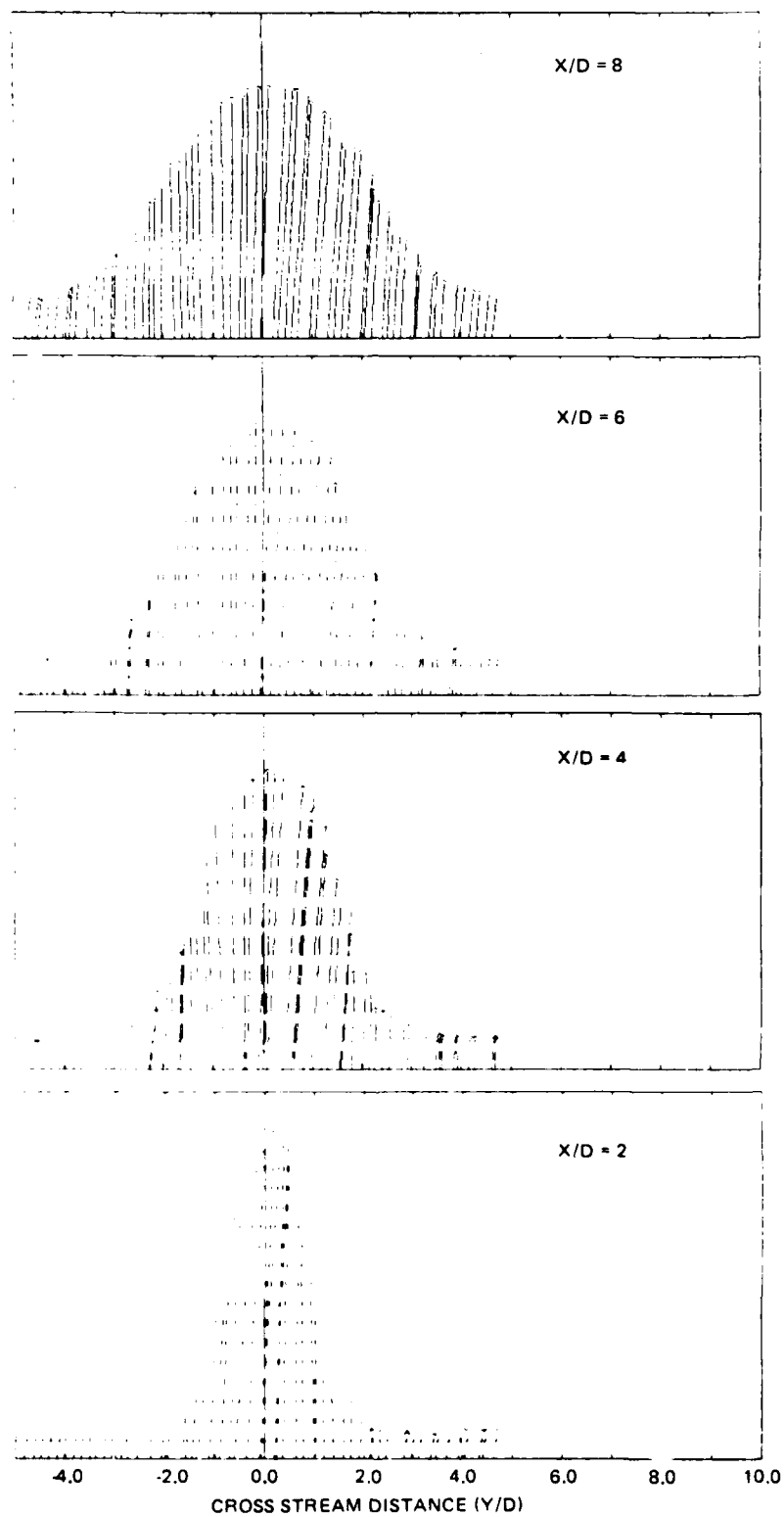
In an attempt to explain the increased turbulence mixing rate found in the upwash, several types of experiments were performed to examine the effect of the initial wall jet conditions on the upwash. These include a series of experiments using unequal strength source wall jets, another series utilizing various height obstacles or fences located at the collision point of equal strength wall jets, and a series using tape boundary layer trips to assure turbulent wall jets.

A series of experiments was conducted using different source jet pressures. The pressure ratios were 1.0, 1.2, 1.4, 1.6 and 1.8, and profiles were taken at heights of 2, 4, 6 and 8 wall jet half heights used in the equal jet case. This combination of wall jet pressures and profile heights was selected because of the physical constraints of the test facility. The data acquisition and processing procedure was the same used in the equal jet case. The short version of the program was used.

Figures 21 through 25 show the mean velocity vector profiles for these cases. Using the magnitude of the mean velocity, we again computed the half velocity growth rates from a Gaussian curve fit. These are shown in Fig. 26. It is interesting that all of these curves converge to approximately $B/D = 1$ at $X/D = 2$, implying that the extent of the collision zone is approximately two characteristic heights.

The required linear decay rates of the inverse maximum velocity squared curves are shown in Fig. 27. These curves are normalized by the maximum source jet velocity squared. For equal jets this is proportional to one half the total source momentum. By normalizing the curves by the average source momentum, the curves become almost identical with a slightly higher decay rate (larger slope) for the more unequal jet case.

Figure 28 shows the locus of the centerline points for each case examined. These are plotted with respect to the physical centerline of the apparatus. Linear curve fits give the slope of the upwash and the intercept point on the ground plate. A simple analysis, presented in the next section, gives an estimate of these values. The slopes are predicted very well in this



1335-014D

Fig. 21 Upwash Flow Field Vectors for Pressure Ratio = 1.0

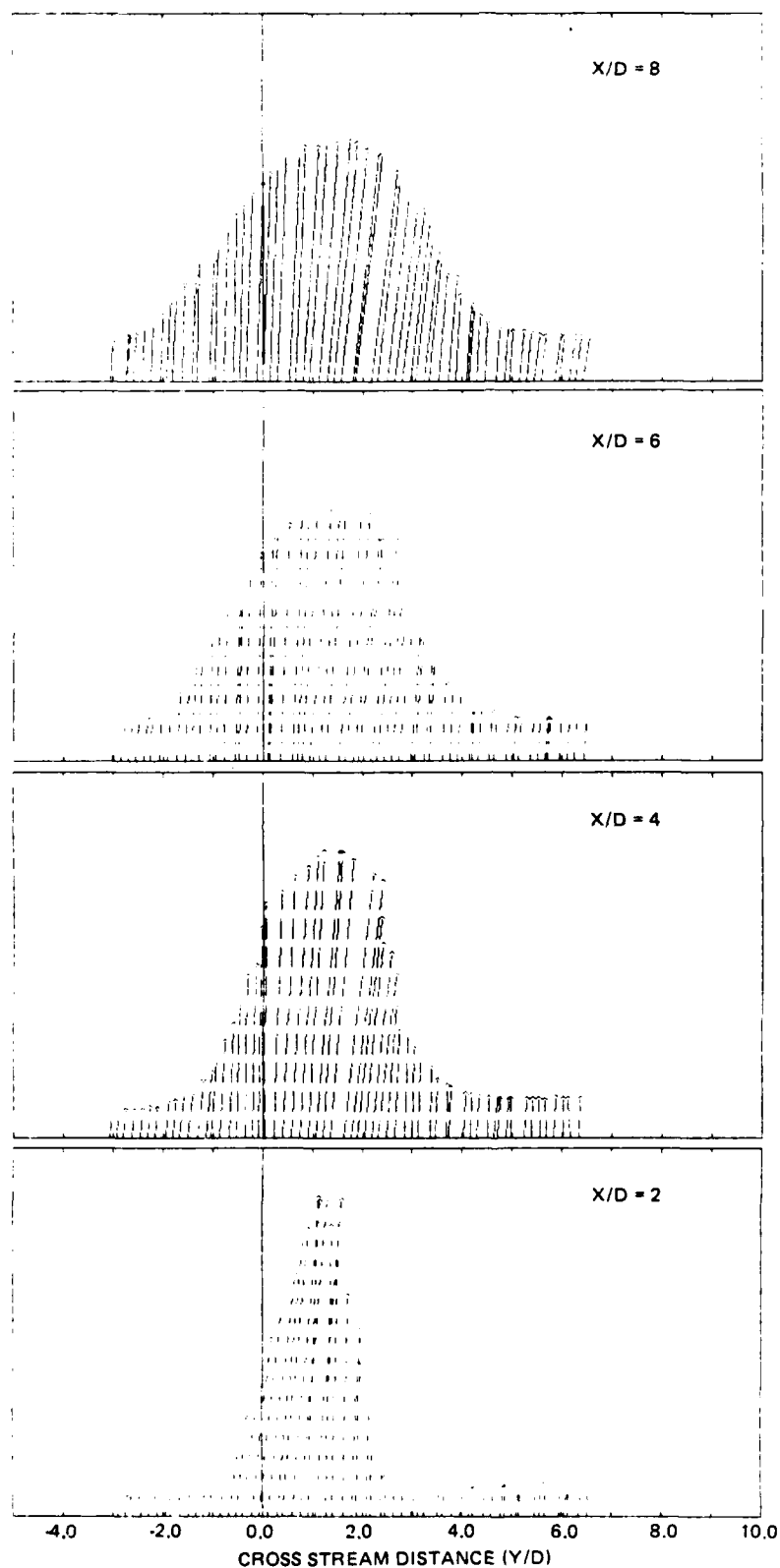


Fig. 22 Upwash Flow Field Vectors for Pressure Ratio = 1.2

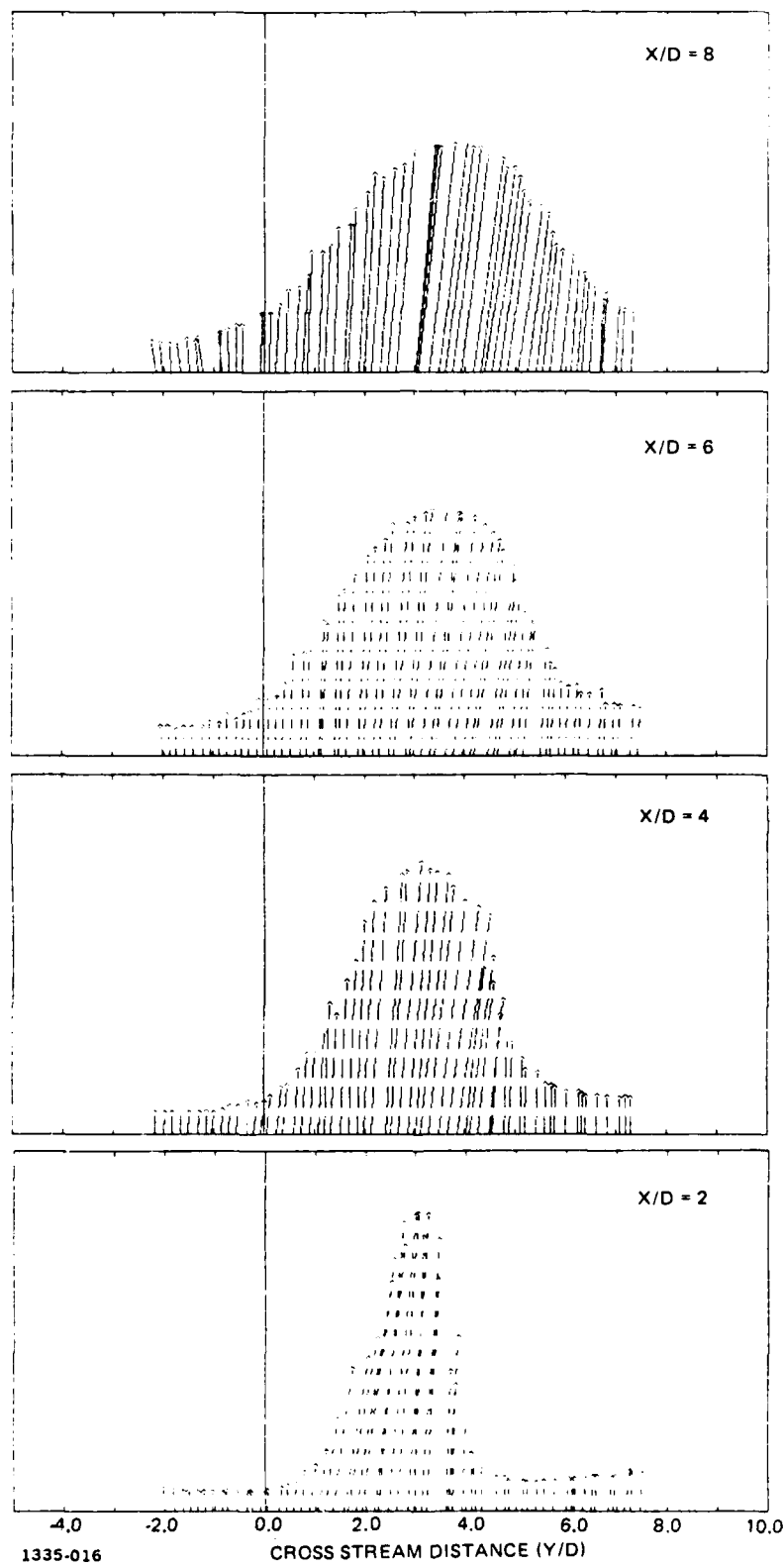
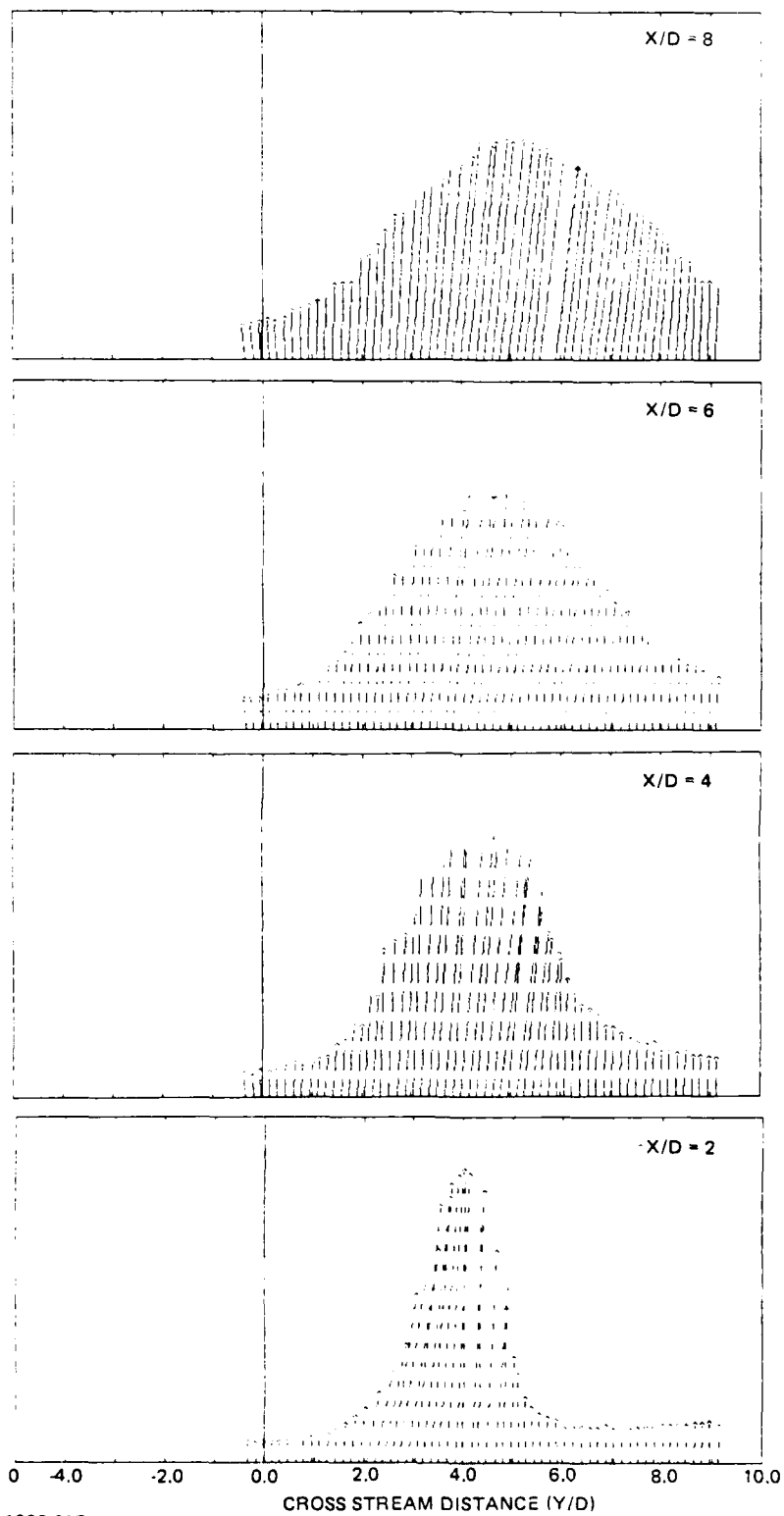
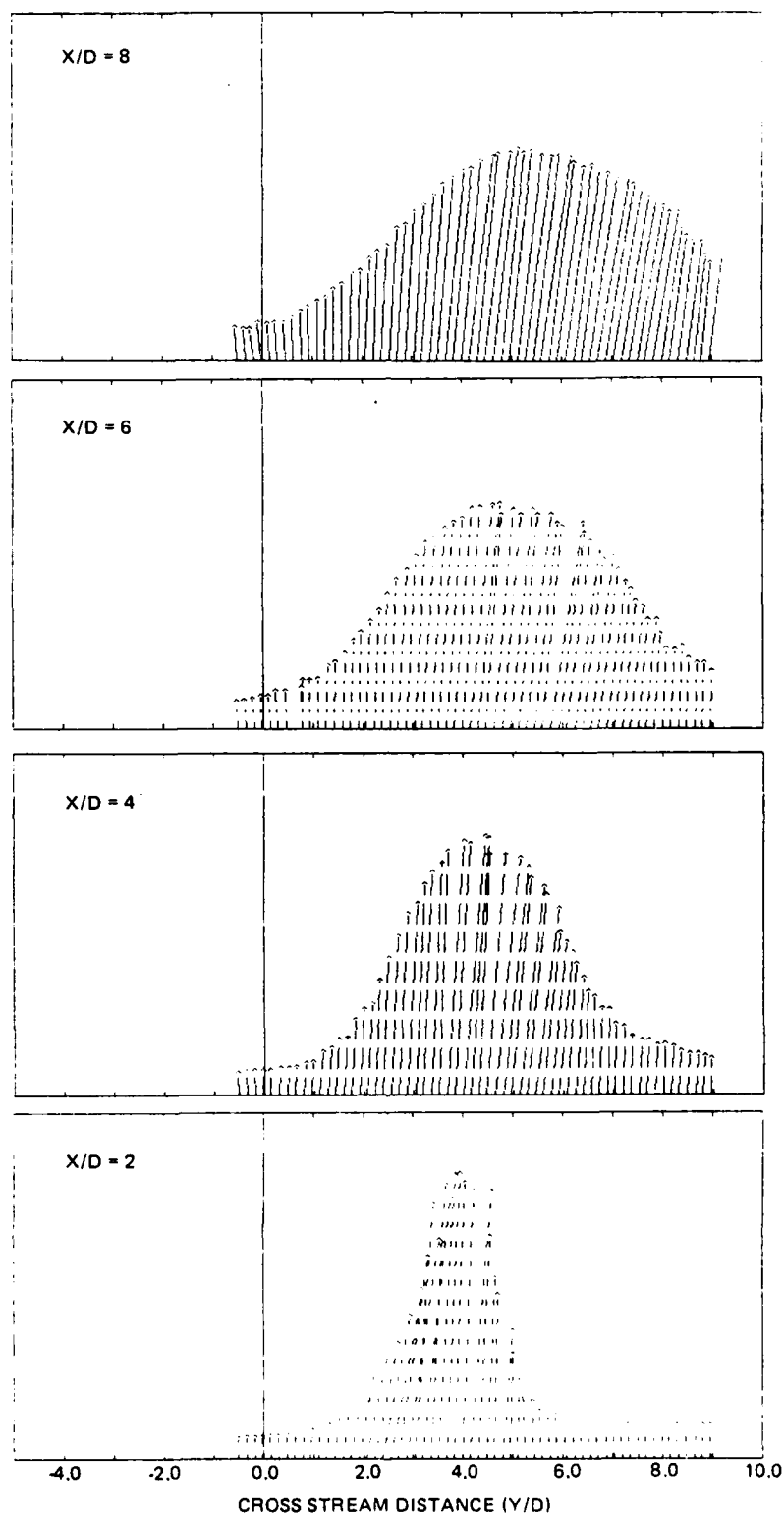


Fig. 23 Upwash Flow Field Vectors for Pressure Ratio = 1.4



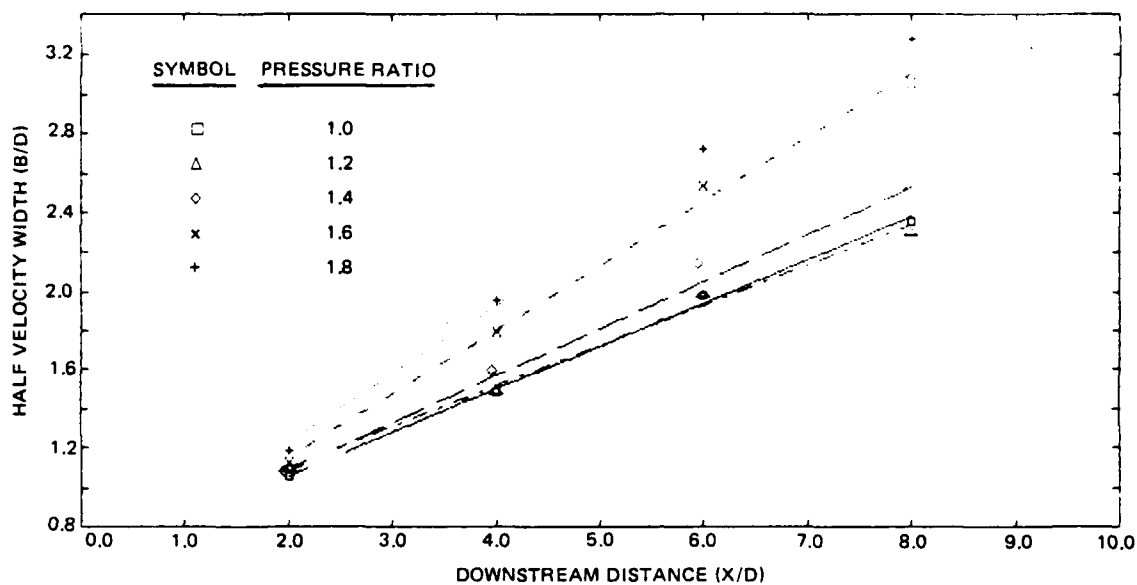
1335-017D

Fig. 24 Upwash Flow Field Vectors for Pressure Ratio = 1.6



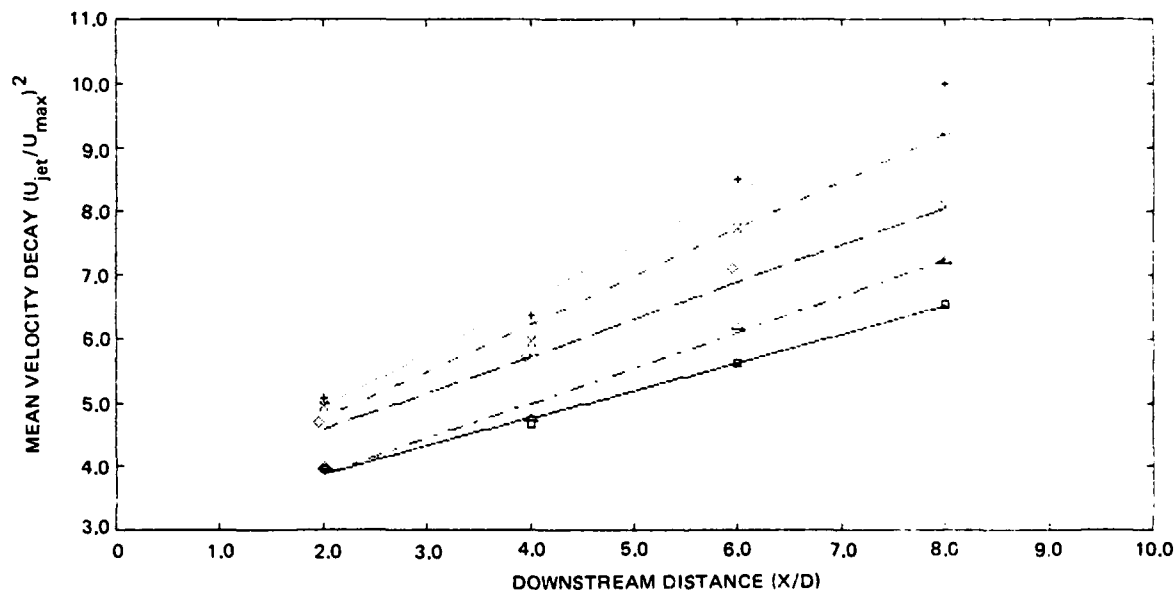
1335-018D

Fig. 25 Upwash Flow Field Vectors for Pressure Ratio = 1.8



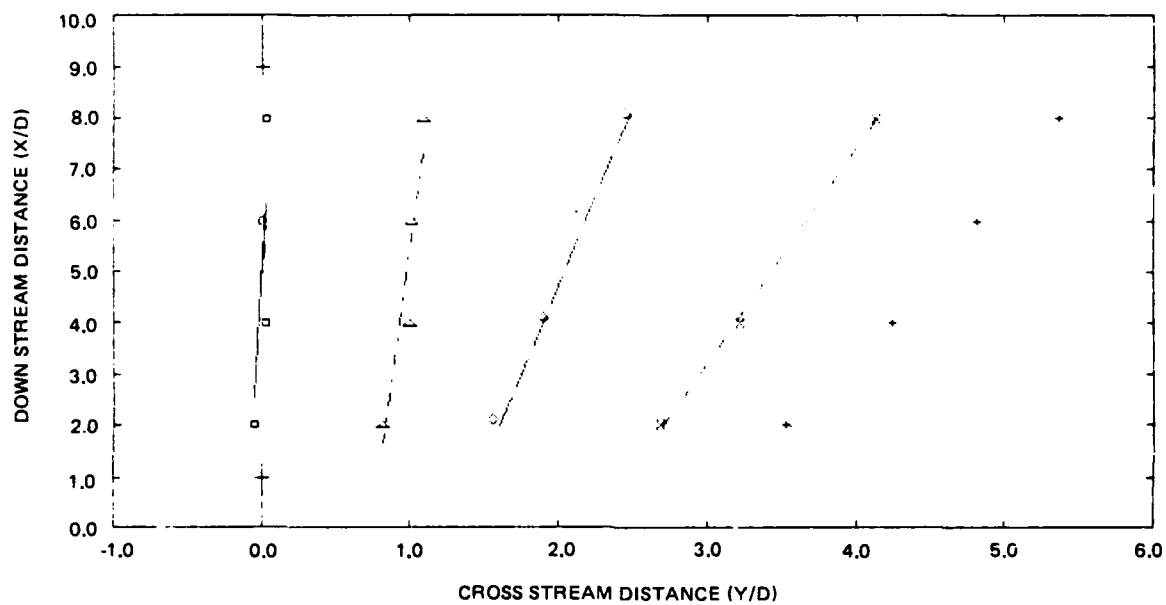
1335-019D

Fig. 26 Half Velocity Width Growth Rate in the Upwash of Unequal Wall Jets



1335-020D

Fig. 27 Mean Velocity Decay in the Upwash of Unequal Wall Jets
(See Fig. 26 for Symbol Key)



1335-021D

Fig. 28 Position of the Maximum Velocity Peak in the Upwash of Unequal Wall Jets
(See Fig. 26 for Symbol Key)

simple analysis, but the intercept is, in all cases, underpredicted. This is easily explained when one considers that the upwash is formed from the top of the collision bubble and necessarily, the extrapolation to the plate will underpredict (i.e., indicate a location closer to the centerline) the origin point (see Fig. 30). Many of the derived values are summarized in Table I.

Figure 29 shows the turbulent kinetic energy normalized by the local maximum mean velocity. These profiles have been shifted in space so that they are all plotted with respect to their individual centerlines. This has the effect of plotting the profiles along a centerline in the direction of the upwash. The higher speed jet is from the left.

There are two features of these profiles that distinguish them from the equal jet case. While it is not obvious from the mean profiles, it was expected that the thinner wall jet from the right would produce a slightly higher shear rate right of center at the lower developing stations. The result of the greater shear is greater turbulence generation, which is seen in these profiles. In addition, due to the relatively smaller mass flow from the right, it was expected that the maximum velocity point would be right of the symmetry point but would migrate towards the center as the flow developed. The data confirm this expectation. The small data scatter at the lowest station is due to increased weighing of the v component in the energy calculation (see Fig. 11-14). The Reynolds stress data, not shown here, exhibit the typical zero crossing at the centerline with decreasing maxima with increasing pressure ratio. At the lowest station, the left hand side shows a noticeable decrease in shear stress. This is a behavior contrary to simple mixing length theory and is in our view due primarily to the large cross stream turbulent energy component remaining from the collision process.

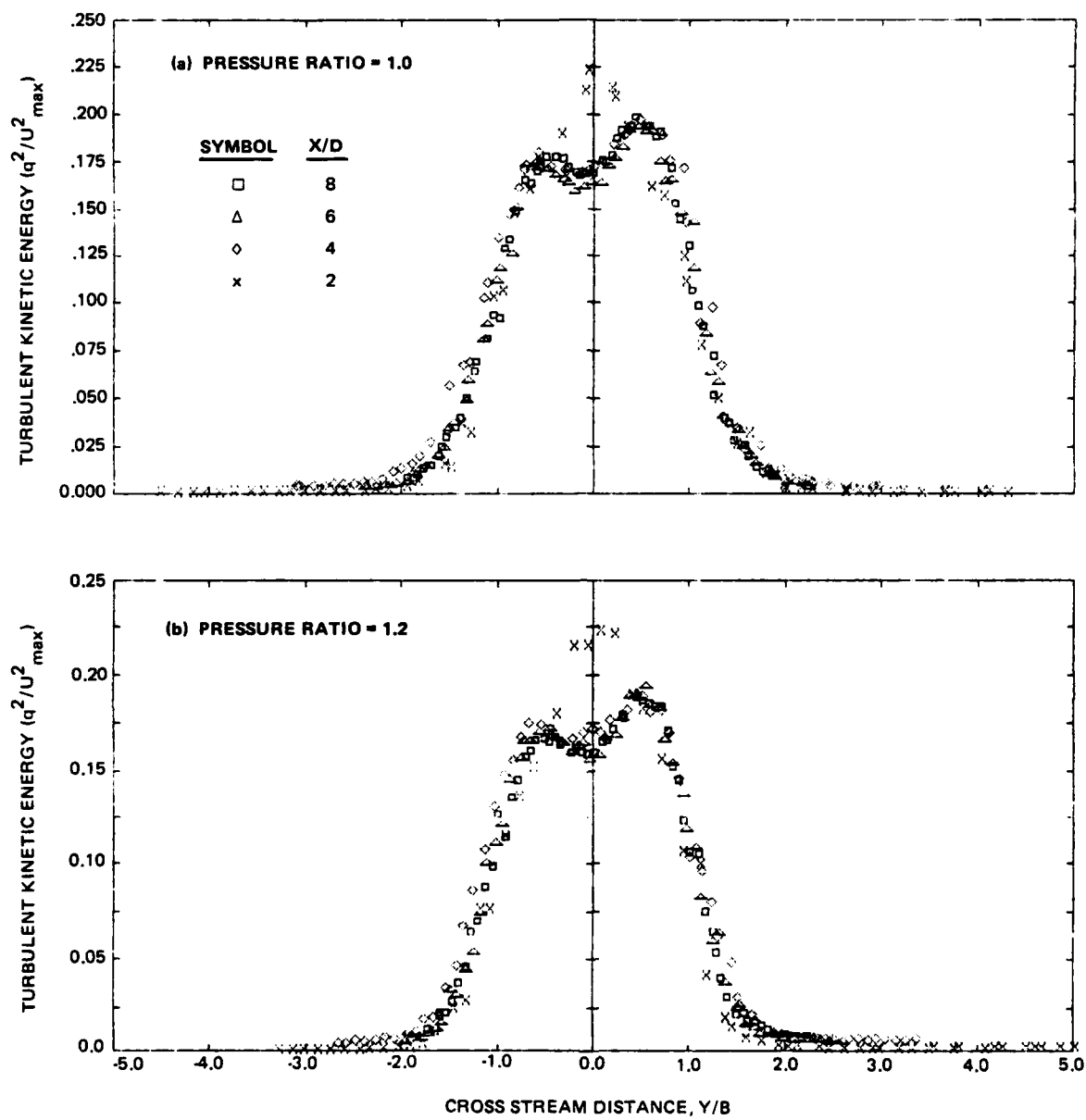
UNEQUAL JET ANALYSIS

By means of a very simplified analysis, the position of collision and the angle the upwash makes with the ground plane may be estimated. This analysis employs integral mass and momentum balances about a control surface around the collision point. Denoting flow from the left as 1, the right as 2, and exiting as 3 (as shown in Fig. 30) gives mass

$$m_1 + m_2 = m_3 \quad (1)$$

and momentum

$$h_1 u_1^2 - h_2 u_2^2 = h_3 u_3^2 \cos \theta. \quad (2)$$



1335-022D(1/2)

Fig. 29 Turbulence Kinetic Energy in the Upwash of Unequal Wall Jets (Sheet 1 of 2)

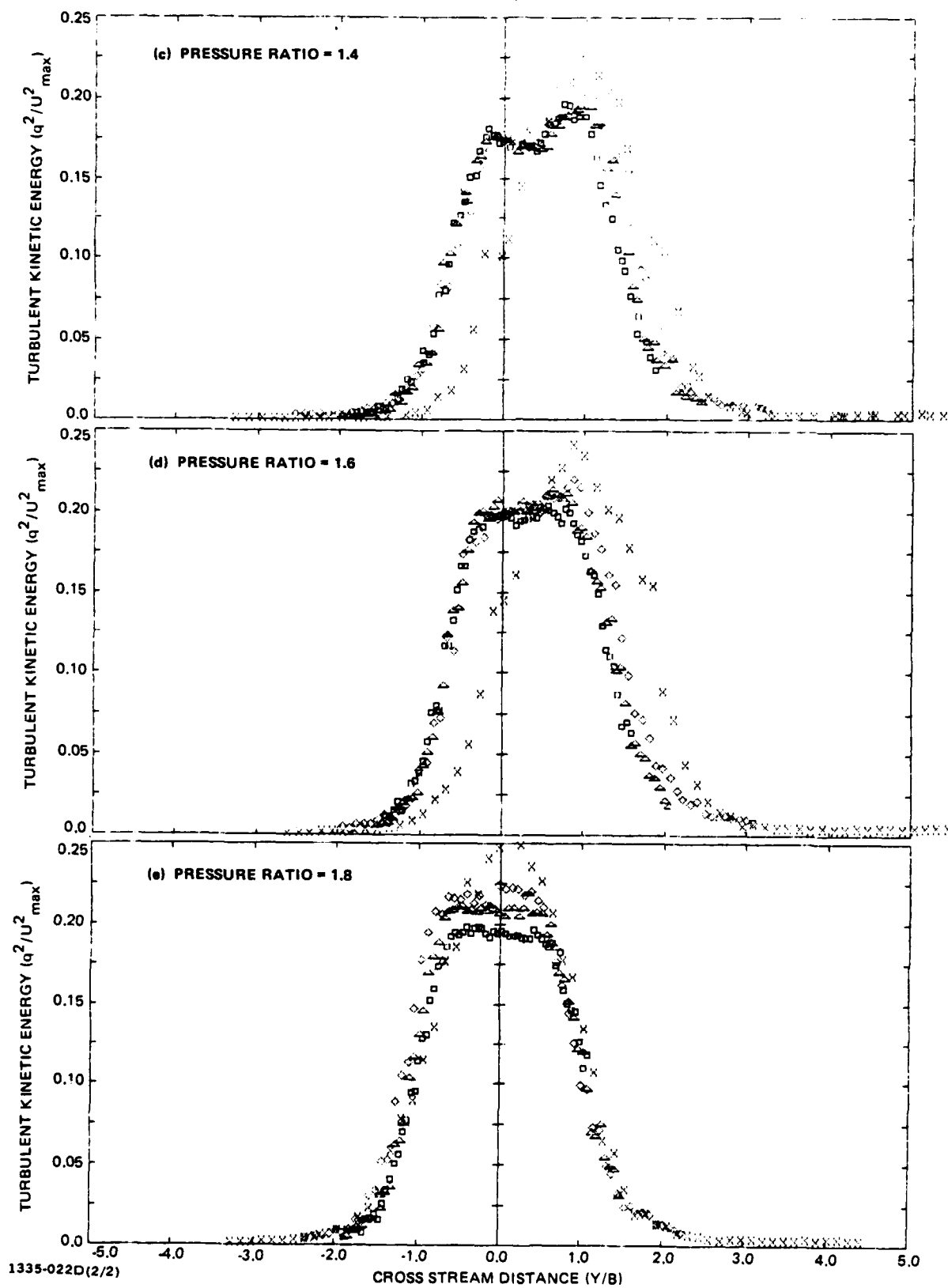
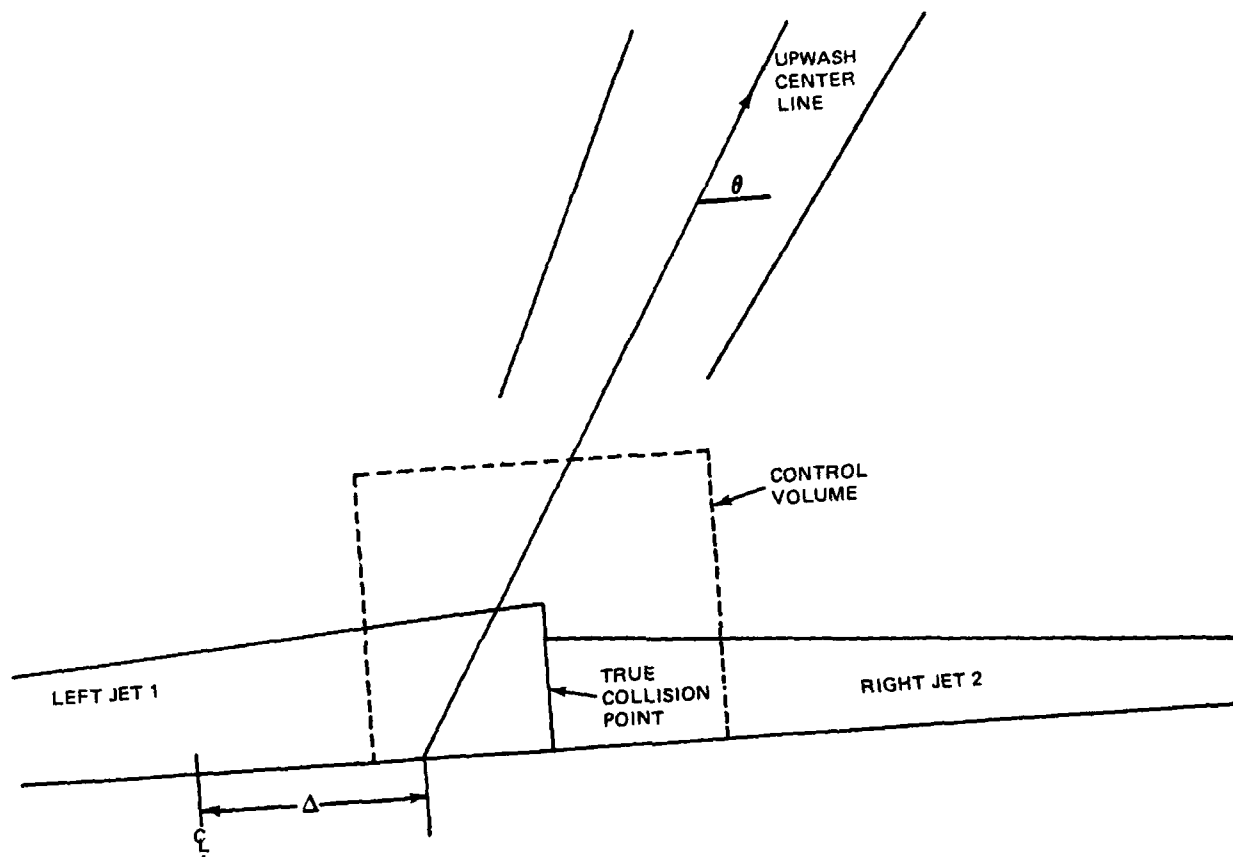


Fig. 29 Turbulence Kinetic Energy in the Upwash of Unequal Wall Jets (Sheet 2 of 2)



1335-023D

Fig. 30 Unequal Wall Jet Diagram

TABLE I

Pressure Ratio, K	Distance from CL to Collision (Δ/D)		Upwash Angle		Growth Rate	Decay Rate	Normalized Decay Rate
	Predicted	Measured	Predicted	Measured			
1.0	0	-0.05	90.0	88.7	0.220	0.443	0.443
1.2	1.11	0.77	85.4	87.2	0.207	0.558	0.513
1.4	2.04	1.31	81.4	81.7	0.240	0.577	0.498
1.6	2.99	2.23	77.4	76.5	0.326	0.741	0.600
1.8	3.69	2.97	74.4	73.1	0.353	0.843	0.655

See Fig. 30

Now assume, based on observation, that the point of collision is where the total pressures from each side are equal, that is,

$$\begin{aligned} 1/2 \rho u_1^2 &= 1/2 \rho u_2^2 \\ u_1^2 &= u_2^2 \end{aligned} \quad (3)$$

Since this is a simple analysis, the following proportionalities will be used:

$$\begin{aligned} u_1 &\sim u_{1,\max} \\ h_1 &\sim b_1 \text{ (the half velocity height)} \\ \text{introducing } K &= \text{ratio of the initial momenta} \\ &= (u_{j1}/u_{j2})^2 \end{aligned} \quad (4)$$

and taking $K > 1$, implying the stronger jet is from the left, and substituting into (3) gives

$$\left(\frac{u_{j1}}{u_1}\right)^2 = K \left(\frac{u_{j2}}{u_2}\right)^2 \quad (5)$$

at the collision point. Now using (4) and (2) with $u_1 = u_2$ at the collision and $u_1 = u_3$ from Bernoulli's equation gives

$$\begin{aligned} b_1 - b_2 &= b_3 \cos \theta && \text{from (2)} \\ b_1 + b_2 &= b_3 && \text{from (1)} \end{aligned}$$

so

$$\cos \theta = \frac{b_1 - b_2}{b_1 + b_2} \quad (6)$$

Now (5) and (6) can be used to determine the position and angle of the upwash flow. The wall jet relationships given in Ref. 8 for growth

$$b/D = 0.651 + 0.0728 X/D \quad \text{and for}$$

decay

$$(U_j/U_{\max})^2 = 0.35 + 0.065 X/D$$

are used in the calculations shown in Table I.

CENTERLINE OBSTACLES

One explanation that has been advanced for the large mixing rate and intermittency factors found in the upwash is a lateral movement of the entire upwash jet. If this were the case, it would be expected that a small object located at the collision point would pin the upwash and thereby reduce the mixing rate. We used six splitter plates located at the collision point. These obstacles are $1/4$, $1/2$, 1, 2, 3 and 4 characteristic wall jet heights and were tested with both jets operating.

All of the profiles are similar to those already shown for equal jets. The only noticeable difference in some of the profiles is the presence of a small centerline dip, due to the wake of the splitter plate, at the lowest location. The results of the curve fit are given in Table II.

It is apparent that an increased growth rate is inherent to two-stream mixing jets where these streams have some head-on component velocities. The increased mixing in the upwash is due directly to the two-stream mixing process. Even with large splitter plates, where the wall jet flow has been turned into the vertical direction, there is still an increased mixing rate over the classical free jet value. For large splitters, the wall jets are nearly re-established before the vertical wall jets meet. At this point, the turning turbulence has started to die out. The resulting growth rate of 0.130 is much less than the upwash jet value of 0.220 but is still more than 0.10 for free jets. However, it is twice the wall jet (one from each side of the plate) value of 0.068. As the plates become smaller, the two-jet influence is more pronounced. It is obvious that lateral solid body motion of the upwash is not necessary for an increased mixing to be observed.

The case labeled "sand" is a test in which sandpaper trips were installed halfway between the jet exit and the centerline. This was done to insure a fully turbulent boundary layer. Since the wall jet dominates the upwash formation, there is no effect in the upwash due to the boundary layer changes. The linear half velocity growth develops a very short distance downstream of the splitter plate. Since physical limitations of the apparatus preclude going more than 8D above the plate, a change in these growth characteristics is possible, but unlikely, with increased distance.

TABLE II

Obstacle Height	Growth Rate	Heights Measured
0	0.230	8,6,4,2
1/4 D	0.182	8,6,4,2
1/2 D	0.174	8,6,4,2
1 D	0.144	8,6,4,2
2 D	0.131	8,6,4,2,1
3 D	0.131	8,6,4,3,1
4 D	0.130	8,6,5
sand	0.226	8,6,4,3

RADIAL WALL JETS

It is our approach to study the upwash effects in increasingly more complex flow geometries. After completion of the two-dimensional upwash phase, we then required the construction of an apparatus to provide a radially spreading wall jet. The characteristics found in the two-dimensional upwash will be examined in this new radial upwash.

The usual method employed for the generation of this sort of wall jet is the impingement of the circular free jets into a ground plane. While this method undoubtedly creates a radial wall jet, in the case of the upwash, it also introduces an additional complication: it is impossible to isolate the effects of the presence of circular free jets on the development of the upwash physically located between them. The downward flowing free jets set up a strongly coupled secondary rotating flow with the upward flowing upwash.

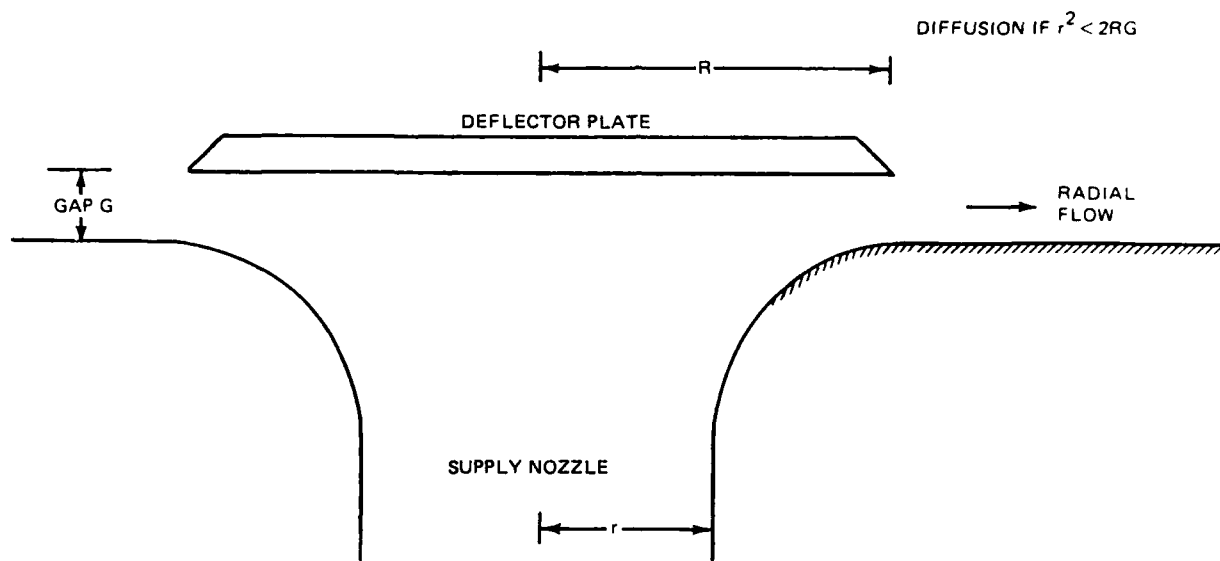
We had to ensure that we had a highly controllable upwash whose characteristics could be studied in a manner de-coupled from other effects. Therefore, a study was undertaken to determine if a radically different geometry could be used to produce a suitable radially spreading wall jet. The geometry chosen was one that employed a circular source jet flowing through the ground plane from below. The circular jet was then diverted into the radial direction along the ground by impinging upon a circular deflector plate. It was found that using a much smaller gap than originally designed produced the desired flow. This design was then used in the full scale test

facility that will be the primary apparatus used in the next follow-on phase. After we complete that phase, the full simulation of the V/STOL upwash will be examined in future follow-ons. This would use an upwash formed from the collision of impinging jets. Some of the development work on the new apparatus will now be reported.

The basic concept of the design is shown in Fig. 31. Several wall jet profiles were obtained from a conventional free jet impingement. These were used to compare with the wall jet profiles measured from the various geometries tested. Mean velocity decay curves and wall jet half height growth rate curves were also compared to assure that the wall jet obtained in the new geometry had the same characteristics as a conventional radial wall jet. Tests were conducted at several gap heights and with deflector plates of three different diameters. Decay and growth characteristics were computed from mean velocity profiles taken at the exit and at least six locations downstream.

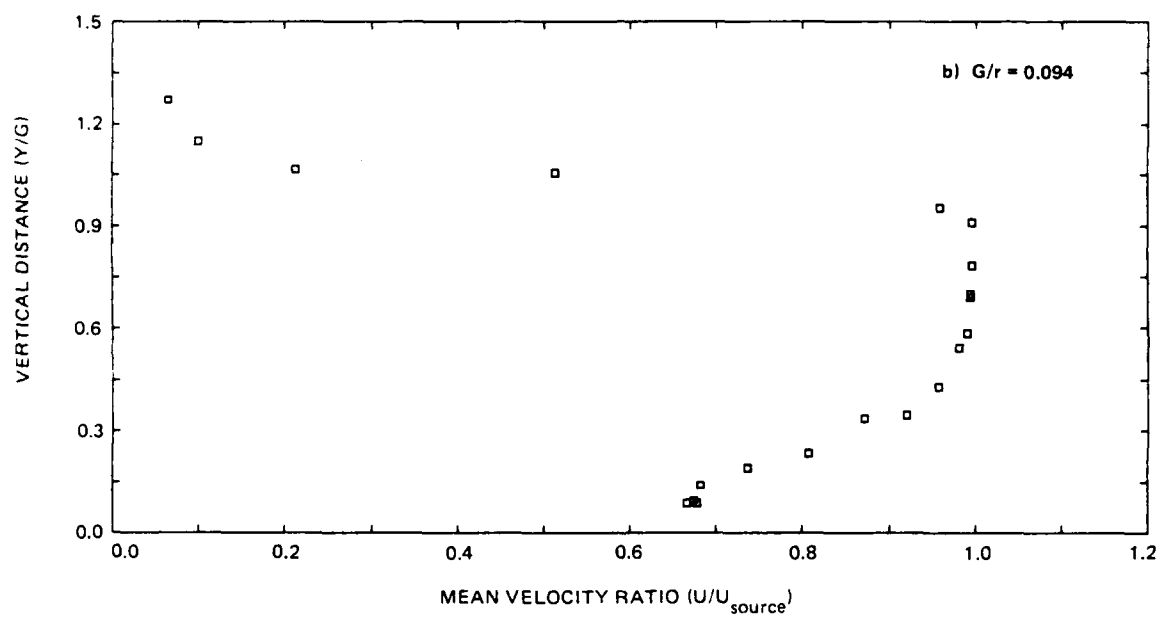
In summary, it was found that if the gap was too large, the wall jet would form on the deflector plate, i.e., it would stick to the wrong surface. An example is shown in Fig. 32. Once this effect was identified, the choice of deflector plates was driven by the desire to minimize the internal diffusion effect as the flow changes direction. The largest radius of curvature supply nozzle available was chosen for the same reason. There is a net diffusion inside the turn if $RG > r^2/2$. In the small gap case, there is a minimum flow cross-sectional area at the nozzle lip, normal to the plate. There is no net diffusion up to this point, only beyond. A separation bubble at the inner nozzle lip could promote downstream problems on the adjacent wall. In the large gap case, there is a minimum flow area in the nozzle, and diffusion area depends on the gap height. The plate was chosen such that the diffusion of the wall jet flow would take place outside of the turn.

Figures 33 and 34 show the normalized mean velocity decay profiles and half width growth rate for acceptable flow geometries. In this form, the decay is independent of the specific arrangement. However, the effect of the internal diffusion on the flow rate is apparent in Fig. 35. The smaller gaps induce more flow. The smallest gap height was chosen for the full scale apparatus. Our selection was based on the best agreement with classical wall jet characteristics. Figure 36 shows the normalized downstream development of the mean velocity wall jet profiles.



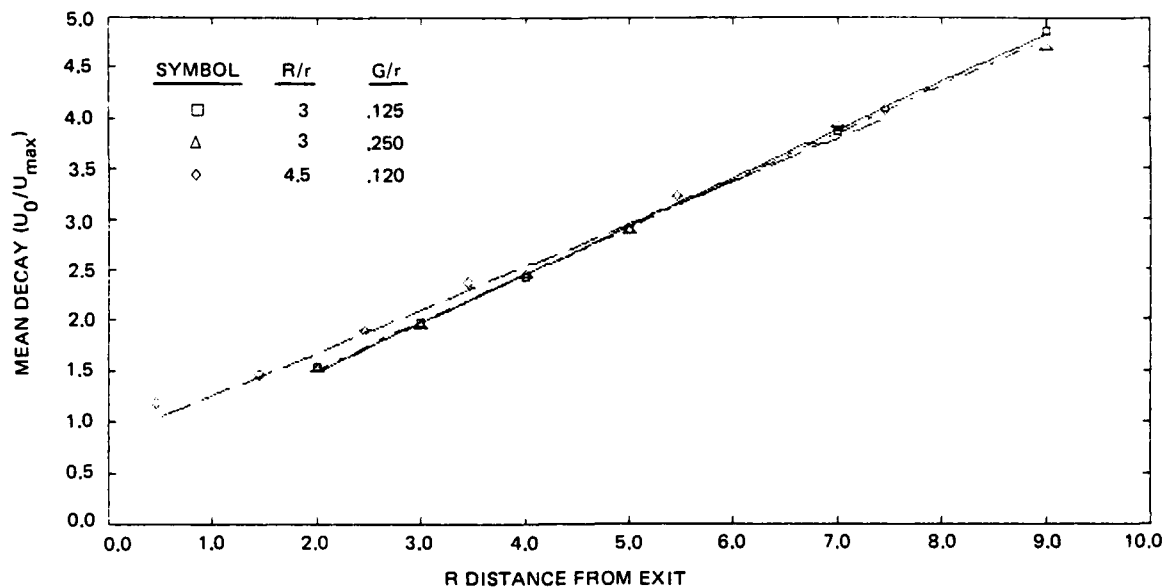
1335-024D

Fig. 31 Diagram of New Radial Wall Jet Design



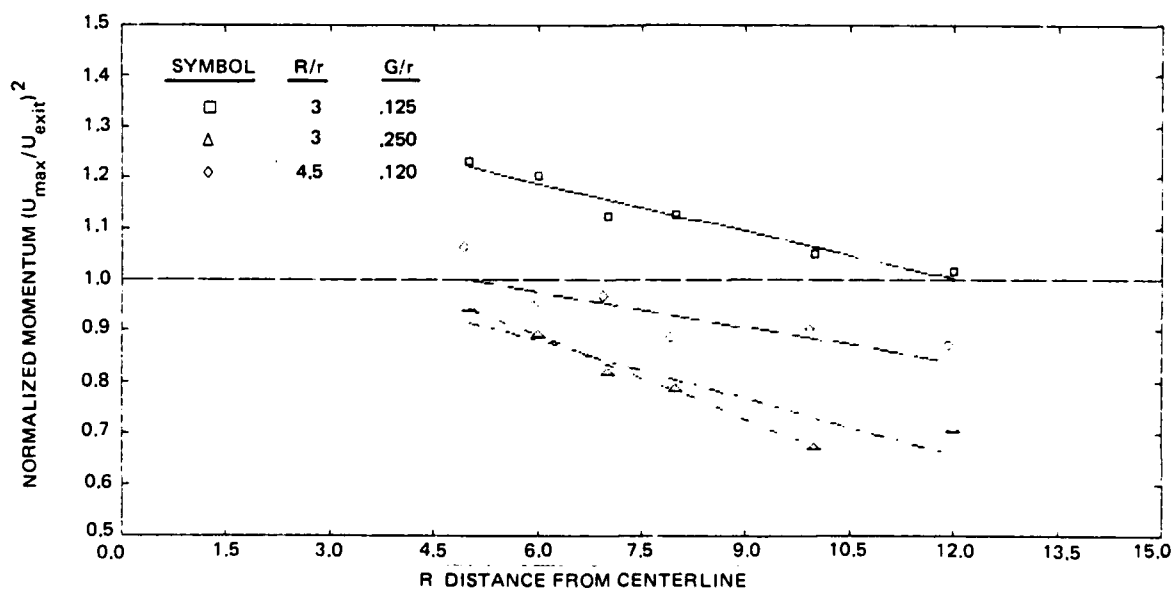
1335-025D

Fig. 32 Radial Wall Jet Exit Profiles



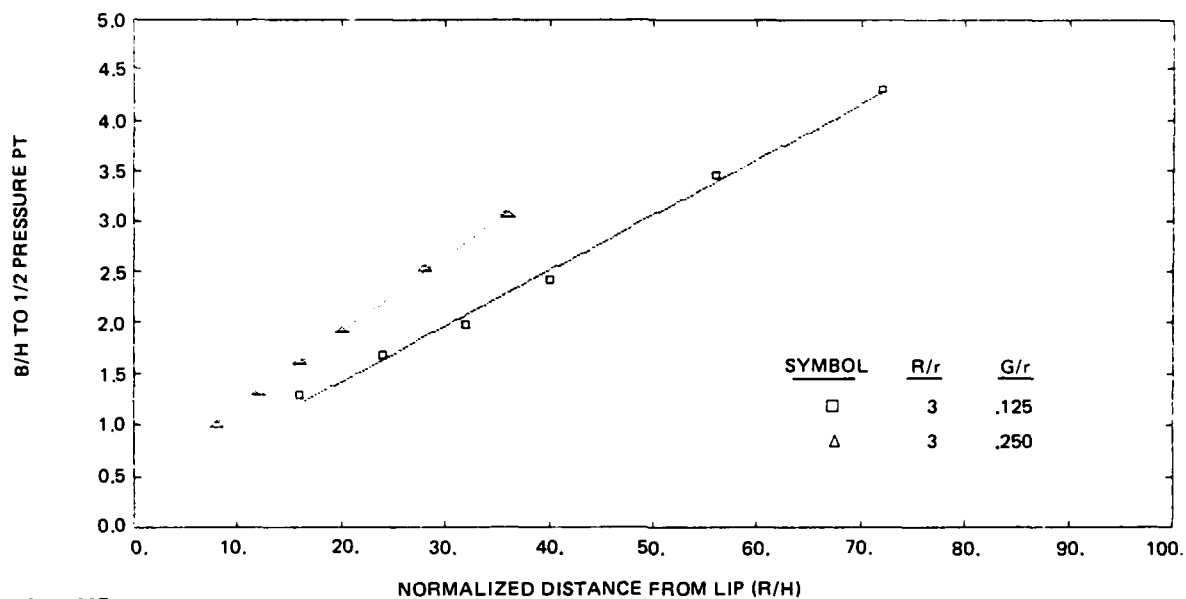
1335-026D

Fig. 33 Radial Wall Jet Mean Velocity Decay Profile



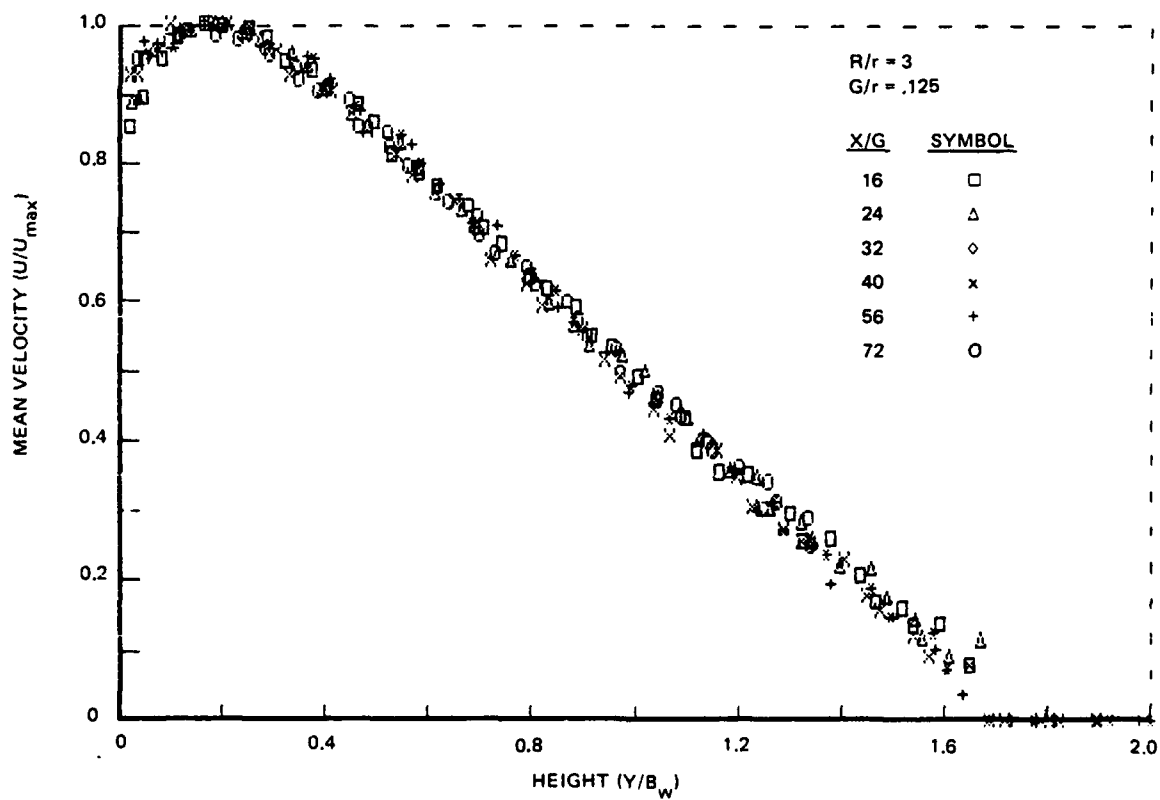
1335-027D

Fig. 34 Radial Wall Jet Momentum for Different Gap Heights



1335-028D

Fig. 35 Increased Mass Flow Rate for Radial Wall Jets



1335-029D

Fig. 36 Radial Wall Jets Mean Velocity Profiles

CONCLUSION

Our experimental investigation of the turbulence mechanisms in a V/STOL upwash field was conducted in a two-dimensional facility to simplify the geometric complexity and interference effects of a real V/STOL flow. The basic turbulence characteristics in the upwash are similar to those found in an ordinary two-dimensional free jet. The most notable differences are the much greater mixing rate and turbulence scale (shown by the intermittency) in the upwash. The higher mixing rate is explainable primarily on the basis of the head-on collision and turning effect of the wall jets that form the upwash. These create large turbulent eddies that involve more ambient fluid than normal. Higher rates than these observed by previous investigators are most likely due to a combination of measurement difficulties and poor control of source streams. Higher turbulence levels reported by others seem to be due to misinterpretation of the data. Development of an apparatus for the continued investigation of a more complex upwash formed from the collision of radial wall jets is also described. This unique design assures that the upwash may be studied separately from the effects of source jet impingement and secondary flows. Future work will include the study of the upwash formed from the collision of impinging jets.

REFERENCES

- 1 Rajaratnam, N., Turbulent Jets, Developments in Water Science, 5. Elsevier Scientific Publishing Col., Amsterdam, 1976.
- 2 Harsha, P.T., "Free Turbulent Mixing: A Critical Evaluating Theory and Experiment," AEDC-TR-71-36, Feb 1971.
- 3 Kind, R.J. and Suthanthiran, K., "The Interaction of Two Opposing Plane Turbulent Wall Jets," AIAA Paper No. 72-211, AIAA 10th Aerospace Sciences Mtg, San Diego, CA, 17-19 Jan 1972.
- 4 Witze, P.O. and Dwyer, H.A., "Impinging Axisymmetric Turbulent Flows: The Wall Jet, The Radial Jet and Opposing Free Jets," Symp on Turbulent Shear Flows, Vol 1, 23-30 April 1977, Univ Park, PA.
- 5 Kotansky, D.R. and Glaze, L.W., "The Effects of Ground Wall-Jet Characteristics on Fountain Upwash Flow Formation and Development," AIAA Paper No. 81-1294, AIAA 14th Fluid & Plasma Dyn Conf, 23-25 June 1981, Palo Alto, CA.
- 6 Foley, W.H. and Finley, D.B., "Fountain Jet Turbulence," AIAA Paper No. 81-1293, AIAA 14th Fluid & Plasma Dyn Conf 23-25 June 1981, Palo Alto, CA.
- 7 Jenkins, R.A. and Hill, W.G., Jr., "Investigation of VTOL Upwash Flows Formed by Two Impinging Jets," Grumman Research Department Report RE-548, Nov 1977.
- 8 Gilbert, B.L., "Detailed Turbulence Measurements in a Two Dimensional Upwash," Paper No. 83-1678 presented at AIAA 16th Fluid & Plasma Dynamics Conf, Danvers, MA, 12-14 July 1983.
- 9 Hill, W.G., Jr. and Jenkins, R.C., "Effects of Nozzle Spcing on Ground Interference Forces for a Two-Jet V/STOL Aircraft," AIAA Paper No. 79-1856, AIAA Aircraft Systems and Technology Conf, NY, 20-22 Aug 1979.
- 10 Hill, W.G., Jr., Jenkins, R.C. and Gilbert, B.L., "Effects of the Initial Boundary Layer State on Turbulent Jet Mixing," AIAA J., Vol 14, No. 11, Nov 1976, pp 1513-1514.
- 11 Kline, S.J. et al., ed, Proc of the 1980-81 AFOSR-HTTM-Stanford Conf on Complex Turbulent Flows, published by Stanford University, CA, 1981.

- 12 Townsend, A.A., The Structure of Turbulent Shear Flow, second ed,
Cambridge University Press, Great Britain, 1980.

PUBLICATIONS FROM THIS CONTRACT

"Detailed Turbulence Measurements in a Two Dimensional Upwash," Paper No. 83-1678 presented at the AIAA 16th Fluid & Plasma Dynamics Conf, Danvers, MA, 12-14 July 1983.

PERSONNEL

The research has been carried out by the staff of the Grumman Aerospace Corporation R&D Center. Dr. Barry Gilbert has been the Principal Investigator, reporting to Mr. Vincent Calia, Laboratory Head of the Experimental Fluid Dynamics Laboratory, and Dr. Richard Oman, Director of Aerosciences. Dr. Gilbert devoted approximately 80% of his time to this contract. Some additional research support was provided by Mr. Richard C. Jenkins, Senior Research Scientist, who conducted most of the radial wall jet testing. The research has benefited greatly from many discussions and interactions with Dr. Arthur Rubel, Laboratory Head of Theoretical Aerodynamics, who provided insights from the viewpoint of V/STOL interaction theory.

END

FILMED

2-85

DTIC